UNIVERSITÀ DEL PIEMONTE ORIENTALE

DEPARTMENT OF HEALTH SCIENCES

SCHOOL OF MEDICINE

Master's degree in Medical Biotechnologies

Evaluating the functional role of cancer cell-derived full-length Factor VIII

Supervisor

Prof. Antonia FOLLENZI

Firmato digitalmente da Antonia Follenzi
Data: 28.09.2026 23:37:43 CEST
Organizzazione: UNIVERSITA' DEGLI STUDI DEL PIEMONTE ORIENTALE/01943490027

Candidate

Seemab Yusuf Shaikh

Co-supervisor

Dr. Gillian E. Walker

Matricula: 20063702

Academic year: 2025/2026

TABLE OF CONTENTS

1. SUMMARY 4

2. INTRODUCTION 5

2.1 Cancer and haemostasis 5

2.1.1 Hemostasis 5

2.1.2 Cancer associated coagulopathy 7

2.1.3 Coagulation factors and cancer 8

2.1.3.1 Tissue Factor 8

2.1.3.2 Factor VIII 8

2.2 Molecular structure of FVIII and its processing 9

2.2.1 Molecular structure 9

2.2.2 Processing of Factor VIII 10

2.2.2.1 Synthesis and intracellular trafficking 10

2.2.2.2 Post-translational modification (PTM) and secretion 11

2.2.2.3 Proteolytic cleavage and activation 11

2.3 The function of FVIII 11

2.3.1 Hemophilia A 12

2.3.2 Extrahemostatic roles of FVIII 12

2.3.2.1 Endothelial cells 12

2.3.2.2 Bone 13

2.3.2.3 Macrophage polarization 13

2.4 Evidence to support a role for FVIII in the pathophysiology of cancer 13

2.4.1 Cancer cell FVIII production 14

2.4.2 Direct effect of FL-FVIII 16

3. OBJECTIVE 17

4. MATERIAL AND METHODS 18

4.1 Cell culture and treatment 18

4.2 Lentiviral (LV) transduction 18

4.3 Quantification of transduction efficiency by FACS 19

4.4 Integrated Vector copy number (VCN) analysis 20

4.5 RNA extraction and RT-qPCR analysis of FVIII expression 20

4.6 Live-cell imaging for proliferation and survival 21

4.7 Colony-forming assay (CFA) 22

4.8 Migration Assay 22

4.9 Protein extraction and western blot analysis 22

4.10 Statistical analysis 23

5. RESULTS 24

5.1 Cancer cell lines selection and characterization to investigate the function of cell-derived FL-FVIII 24

5.1.1 Ovarian cancer cell lines selected to study the effect of FVIII-FL production 24

5.1.2 Establishing the lentiviral transduction efficiency in A2780, IGROV1 and SKOV3 cells using LV-PGK-GFP 25
5.1.3 Optimization of puromycin selection for stable transduction 27
5.2 Generation and validation of the ovarian cancer cells producing FVIII 28
5.2.1 Generation of A2780 and IGROV1 cells producing cell-derived FL-FVIII 28
5.2.1.2 Vector copy number confirms dose-dependent lentiviral integration 29
5.2.1.2 The FVIII mRNA highlights a variable expression unrelated to VCN 29
5.2.1.3 An inverse FVIII secretion pattern to VCN for FL-FVIII expressing ovarian cancer cells 30
5.3 Pathophysiological assessment of FL-FVIII producing A2780 and IGROV1 cells 31
5.3.1 Proliferation is not influenced by an increase is cell-derived FL-FVIII production, while metabolic overloading has a negative impact. 31
5.3.2 Migration is not influenced by an increase is cell-derived FL-FVIII production 33
5.3.3 Cell-derived FL-FVIII has a cell line specific effect on long-term cell survival 34
5.3.4 Cell-derived FL-FVIII shows cell type specific effects on single cell survival over the long-term 35
5.4 Cell-specific signalling mechanisms observed in relationship to FL-FVIII production 36
5.4.1 Cell-derived FL-FVIII production shows cell type-specific alterations for the integrin/FAK pathway as well as TF production 36
5.4.2 Higher FL-FVIII VCN in A2780 cancer cells causes endoplasmic reticulum (ER) stress and decreased Bcl2 survival protein expression 38
6. DISCUSSION 40
7. REFERENCES 44
ACKNOWLEDGEMENTS 52

1. SUMMARY

Rationale of the Study
Cancer-associated thrombosis (CAT) is a major cause of morbidity and mortality in cancer patients. While tissue factor (TF) has been well studied for its oncogenic roles, Factor VIII (FVIII) is only recognized as CAT biomarker rather than an active participant in tumor biology. Recent evidence, however, has shown cancer cell lines directly produce bioactive FVIII. Intriguingly, the secretion pattern also identified in a broad array of cancer cell lines the strong presence of full length FVIII (FL-FVIII). With the demonstration that recombinant FL-FVIII (rFL-FVIII) can promote proliferation, migration, and survival in bladder cancer and osteosarcoma *in vitro* models, the aim of this thesis was to establish whether sustained cancer cell-derived FL-FVIII production could influence the pathophysiology of cancer cells.

Planning of the Study
Origin-specific cancer cell lines for the study were selected based on an assessment of mRNA for both FVIII and TF using the Cancer Cell line Encyclopedia (CCLE) database (https://portals.broadinstitute.org/ccle), and in-house availability. A very low to negative FVIII mRNA and differential TF expression were the selection criteria. Cell lines were assessed for transducibility using lentiviral (LV)-PGK-GFP driven by the phosphoglycerate kinase (PGK) promoter, and puromycin selection. Two cell lines were stably transduced with a LV vector encoding PGK-FL-FVIII (LV-FL-FVIII). Vector copy number (VCN), FVIII mRNA and FVIII secretion were assessed. Functional assays to assess the pathophysiological effects included live-cell imaging, wound healing, and colony-forming assay, together with molecular analyses of signalling proteins to assess the cellular mechanism/s.

Results
The ovarian cancer cell lines, A2780, IGROV1 and SKOV3 met the study criteria, with IGROV1 and SKOV3 expressing high TF mRNA. The A2780 and IGROV1 cells were transduced with LV-FL-FVIII, with VCN reflecting the multiplicity of infection (MOI), highlighting successful transduction. The FVIII mRNA and secreted protein increased for low VCN (VCN≈2) cells, decreasing with higher VCNs (VCN>4). An increase in FL-FVIII produced cell-type specific effects, stimulating A2780 single cell proliferation, while enhancing survival and prothrombotic state by increasing TF production for IGROV1 cells. In contrast, high FL-FVIII VCNs impacted negatively. The pathophysiological effects were supported by FAK/Src phosphorylation in both cell lines, and an increased expression of β1 and β3 integrin and the survival protein Bcl2 for A2780 cells. Due to the decreased FVIII production and negative impact for the high VCN cells, chronic ER stress was suspected. An assessment of uncoupling protein response (UPR) markers including Inositol-requiring enzyme 1α (IRE1α) and eukaryotic Translation Initiation Factor 2 subunit α (eIF2α) activation, as well as the cleavage of the ER stress sensors caspase12 and increased levels of NRF1, confirmed chronic ER stress in both high and low VCN A2780 cells.

Conclusion
This work provides preliminary evidence supporting a potential role for cell-derived FL-FVIII in the biology of the cancer cells, despite the demonstration that LV model is inappropriate due to UPR activation and ER stress. Results show that FL-FVIII could have multiple roles in tumour biology depending on the context of hosts expression and signalling profile. Alternative strategies are needed to raise the production of FL-FVIII without overloading the secretory pathway so as to assess more efficiently the role played by FL-FVIII in the progression of cancer.

2. INTRODUCTION

2.1 Cancer and haemostasis

Cancer is one of the leading causes of death worldwide. According to GLOBOCAN 2022 (https://gco.iarc.who.int/en), approximately 20 million new cases of cancer are recorded in a year with 9.7 million deaths due to cancer. Roughly 1 in 5 people will develop cancer in their lifetime and about 1 in 12 women will die of cancer (Bray et al., 2024).

Thrombosis is the most common complication for cancer patients, and it is associated with a high mortality rate. It was Armand Trousseau in 1865 who first described the association between cancer and thrombosis (Kwaan and Samama, 2019). The term Trousseau's syndrome is often used to describe a thromboembolic event as the first symptom of a malignant disease. Cancer associated thrombosis (CAT) can vary from atrial or venous thromboembolism (VTE) to disseminated intravascular coagulation (DIC). For hematological malignancies, DIC is commonly observed, while VTE is typical for solid tumors. The different types of VTE include acute superficial and deep vein thrombosis (DVT), pulmonary embolism (PE), and splanchnic vein thrombosis (SPVT; Akinbo and Ajay 2023; Prandoni et al., 2005)

2.1.1 Hemostasis

Hemostasis is a highly conserved, multistep process that preserves blood fluidity while restoring vascular integrity after injury (Figure 1; Repetto and De re, 2017). It involves the coordinated interaction of platelets, coagulation factors, the vascular endothelium, and fibrinolytic proteins. Primary hemostasis begins with platelet adhesion to the damaged vessel wall, their activation and aggregation to form a temporary platelet plug. Secondary hemostasis then reinforces this plug through sequential activation of the coagulation system, culminating in thrombin generation and conversion of fibrinogen into a cross-linked fibrin network. Fibrinolysis subsequently limits clot persistence through plasmin-mediated degradation of fibrin. These processes are not strictly sequential; rather, they overlap and are continuously regulated to maintain a balance between clot formation and clot removal (Repetto and De Re, 2017; Falanga et al., 2013).

Disruption of any component of hemostasis may result in excessive bleeding, or increased thrombosis. In fact, a deficiency or dysfunction of coagulation factors causes bleeding disorders such as haemophilia A (HA) and HB, while quantitative or qualitative abnormalities of von

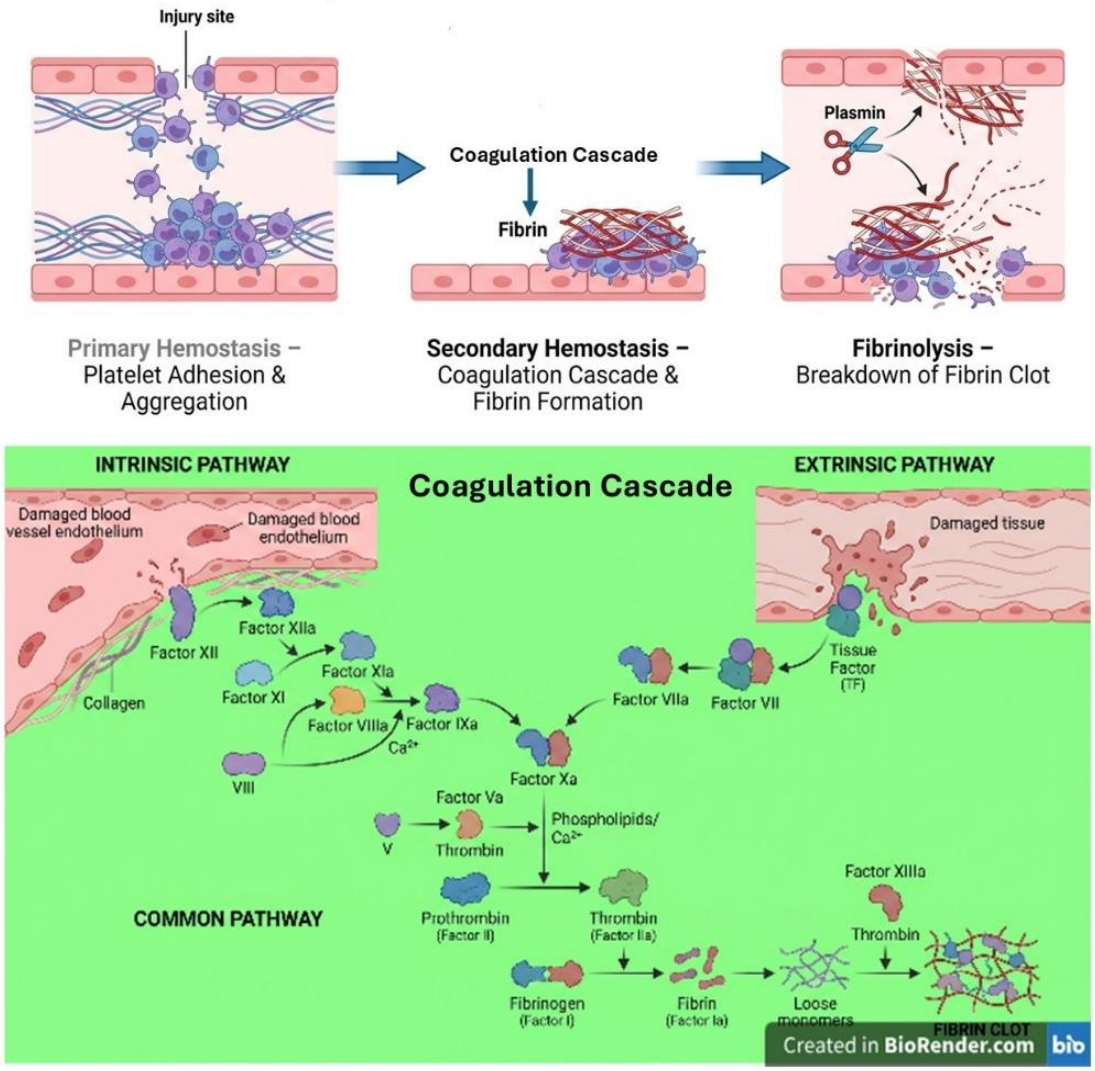


Figure 1: An overview of hemostasis and the coagulation cascade. *(Top panel) Primary hemostasis, secondary hemostasis, and fibrinolysis at the vascular injury site, showing platelet plug formation, fibrin clot formation, and plasmin-mediated clot breakdown. (Bottom panel) The coagulation cascade, showing the intrinsic pathway (initiated by contact activation), the extrinsic pathway (initiated by tissue factor), and their convergence at the common pathway, culminating in thrombin generation and cross-linked fibrin clot formation. (Created with BioRender.com).*

Willebrand factor (vWF), impair platelet adhesion and cause von Willebrand disease (Hui, 2016). Conversely, an inappropriate activation of coagulation may lead to VTE, including DVT and PE (Al-Koussa et al., 2022). Malignancy is a particularly complex cause of hemostatic dysregulation because it may produce both thrombotic and hemorrhagic complications (Goldsmith, 2001, Sheth et al., 2017). While the dominant clinical phenotype is often hypercoagulability, bleeding may occur in advanced disease or in association with thrombocytopenia, disseminated intravascular coagulation, bone-marrow involvement, liver dysfunction, or anticancer treatments (Goldsmith, 2001; Repetto and De Re, 2017).

2.1.2 Cancer associated coagulopathy

Cancer-associated coagulopathy arises from bidirectional communication between malignant cells and the host hemostatic system. Tumor growth, tissue injury, inflammation, surgery, immobility, and systemic anticancer therapies can all contribute to this process (Falanga et al, 2013). Tumor cells and cells within the tumor microenvironment release procoagulant mediators and inflammatory signals that activate platelets, leukocytes and endothelial cells (EC; Figure 2; Ivanciu and Stalker, 2015). In parallel, inflammatory cytokines can induce endothelial activation, increase cellular adhesion, and reduce the anticoagulant and fibrinolytic properties of the vascular surface. This shifts the circulation toward thrombin generation, fibrin deposition, and thrombus formation (Falanga et al., 2013; Repetto and De Re, 2017).

Several cellular mechanisms reinforce this prothrombotic state. Activated platelets can interact with tumor cells and leukocytes, supporting the formation of multicellular aggregates that protect circulating tumor cells and may facilitate their adhesion to the endothelium. Neutrophil extracellular traps, released during NETosis, provide DNA- and protein-rich scaffolds that can promote platelet accumulation, coagulation-factor activation, and fibrin formation. In addition, tumor- and platelet-derived extracellular vesicles can circulate as procoagulant surfaces and may amplify coagulation at sites distant from the primary tumor. These mechanisms are increasingly recognized as components of the link between inflammation, thrombosis and tumor progression, although their relative contribution varies according to tumor type and disease stage (Repetto and De Re, 2017; Sheth et al., 2017).

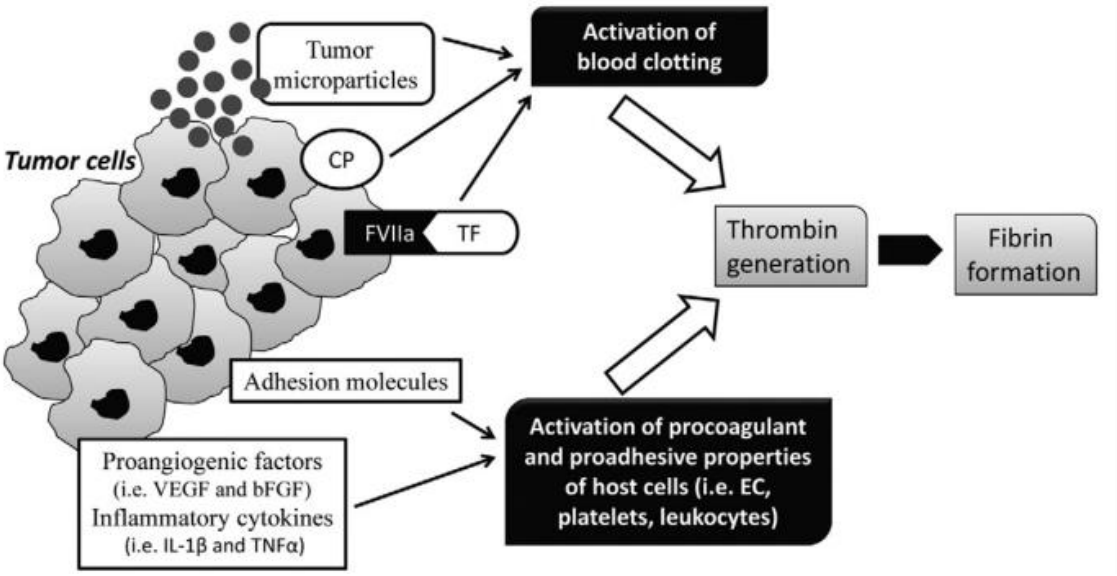


Figure 2: Mechanisms of cancer-associated coagulopathy (Falanga et al. 2013).

Cancer-associated coagulopathy also involves altered fibrinolysis and natural anticoagulant pathways (Winther-Larsen et al., 2022). Increased plasminogen activator inhibitor-1 (PAI1) may suppress plasmin generation and delay clot breakdown, producing a hypofibrinolytic phenotype in some malignancies. However, advanced cancer and disseminated intravascular coagulation may instead result in simultaneous activation and consumption of coagulation factors, increased fibrin turnover and bleeding (Goldsmith, 2001).

2.1.3 Coagulation factors and cancer

Coagulation factors including Tissue Factor (TF), and an emerging player Factor VIII (FVIII), function as potent signalling molecules that shape the tumor microenvironment (TME), promote angiogenesis, and facilitate metastatic dissemination (Claussen et al., 2016; Tamura et al., 2022).

2.1.3.1 Tissue Factor

Tissue Factor, a 47-kDa transmembrane glycoprotein, serves as the primary initiator of the extrinsic coagulation cascade by binding to activated factor VII (FVIIa; Tamura et al., 2022). The TF-FVIIa complex exerts its oncogenic effects primarily through the activation of protease-activated receptors (PARs), particularly PAR-2 (Schaffner and Ruf, 2009). This signalling axis triggers downstream pathways, including Mitogen-Activated Protein Kinase (MAPK), Phosphoinositide 3-Kinase (PI3K), and Janus Kinase - Signal Transducer and Activator of Transcription (JAK-STAT) pathways, which enhance tumor cell proliferation, survival, and migration (Chanakira et al., 2017). The TF-FVIIa-PAR-2 axis has been shown to induce the release of growth factors and support an invasive, angiogenic phenotype (Chanakira et al., 2017). In fact, a high TF expression has been associated with increased angiogenic activity and more aggressive vascular behaviour in malignant tumors, consistent with its role in supporting tumor progression. In addition, TF-bearing extracellular vesicles and microparticles can enter the circulation and contribute to cancer-associated hypercoagulability, thrombosis, and metastatic niche formation (Hisada et al., 2022).

2.1.3.2 Factor VIII

Tumour cells can directly activate the coagulation cascade through the release of TF and factor X (FX) activators, resulting in elevated circulating levels of factors including FV, FVIII, FIX, and FXI (Winther-Larsen et al., 2022). High levels of FVIII are frequently noted in cancer patients and are recognized as an independent risk factor for VTE in this population (Franchini

et al., 2009; Falanga et al., 2003). Hematological cancers produce high levels of FVIII while being void of TF expression showing this increase in FVIII is not necessarily dependent on TF (Mohren et al., 2016). Traditionally viewed as an essential cofactor for activated FIX (FIXa in the coagulation pathway, FVIII has recently been implicated as a direct tumor cell survival factor with metastatic potential (Walker et al., 2025; Prasannan et al., 2025). Since the cloning of the F8 gene in the 1980s, the molecular understanding of FVIII has evolved significantly, revealing a protein of remarkable complexity in its structure, biosynthesis and regulation, supporting a role in cancer (Zhou et al., 2023).

2.2 Molecular structure of FVIII and its processing

2.2.1 Molecular structure

Factor VIII is a complex, high-molecular-weight glycoprotein coded by F8 gene located near the terminus of the long arm of the X chromosome (Thompson, 2003). It contains 26 exons that code for a signal peptide and a 2332 amino acid (aa) polypeptide with three different types of domains (A, B, C), specifically A1-A2-B-A3-C1-C2. (Figure 3; Thompson, 2003; Banerjee et al. 2011). The A domains (A1, A2, A3) each consist of approximately 330aa and share significant homology with ceruloplasmin, a copper-binding protein (Thompson, 2003). The C domains (C1, C2) each contain about 150aa and are homologous to the discoidin-like domains found in other proteins (Thompson, 2003). The B domain is unique, comprising nearly 40% of the total protein (983 residues) and is heavily glycosylated. Finally, the "a" region (a1, a2, a3) are short acidic segments that play crucial roles in FVIII activation and binding, particularly the a3 region which is involved in vWF interaction. (Saenko et al., 2002)

In the circulation, FVIII primarily exists as a metal-bridged heterodimer. This heterodimer consists of:

1. Heavy Chain (HC): Comprising the A1 and A2 domains and varying portions of the B domain (A1-A2-B). The size of the heavy chain varies from 90 kDa to 200 kDa depending on the degree of B-domain proteolysis (Banerjee et al., 2011; Fulcher et al., 1985)
2. Light Chain (LC): Comprising the A3, C1, and C2 domains, with a molecular mass of approximately 80 kDa (Banerjee et al., 2011; Hamer et al., 1987).

It is the association of the HC and LC that is essential for the stability and cofactor activity of FVIII. Despite its size, the B domain is dispensable for coagulant activity (Toole et al., 1986). While both full-length FVIII (FL-FVIII) and B-domain-deleted FVIII (BDD-FVIII) can function as cofactors in the Xase complex, they are not biologically interchangeable. The B domain retained by FL-FVIII influences folding, intracellular trafficking, secretion efficiency, and interactions with chaperones and lectins, and may also modulate contacts with cell-surface or extracellular matrix (ECM) components. Consequently, FL-FVIII and BDD-FVIII can differ in their biosynthetic handling, stability, and potentially in their extra-hemostatic interactions (Jun et al., 2020).

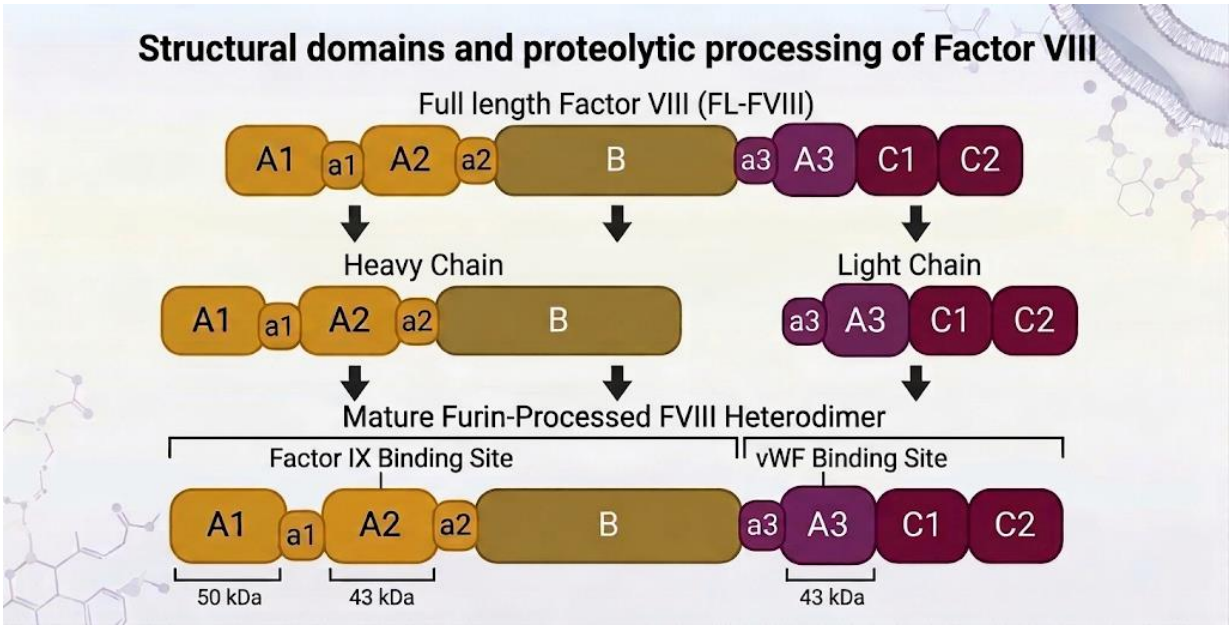


Figure 3: Structural domains and proteolytic processing of Factor VIII (FVIII). Generated using FigureLabs

2.2.2 Processing of Factor VIII

2.2.2.1 Synthesis and intracellular trafficking

The biosynthesis of FVIII is a highly complex and relatively inefficient process, occurring primarily liver sinusoidal endothelial cells (LSECs; Fahs et al., 2014) and hematopoietic cells (Zanolini et al., 2015), though as previously noted, cancer cells can also be a source (Walker et al., 2022). It begins with the synthesis of the 2,351aa precursor in the endoplasmic reticulum (ER). Within the ER, the nascent FVIII polypeptide interacts with several chaperones, such as calnexin, calreticulin, and BiP (immunoglobulin-binding protein), which facilitate proper folding. Successfully folded FVIII molecules are transported to the Golgi apparatus via the

COPII-mediated pathway, a process facilitated by the cargo receptor LMAN1 (ERGIC-53) (Banerjee et al., 2011).

2.2.2.2 Post-translational modification (PTM) and secretion

During its transit through the Golgi, FVIII undergoes extensive post-translational modifications (PTMs). These include N-linked and O-linked glycosylation, occurring primarily within the B domain, which contains 19 potential N-linked glycosylation sites (Banerjee et al., 2011). Tyrosine sulfation at six specific sites (residues 346, 718, 719, 723, 1664, and 1680) is also essential for full procoagulant activity and high affinity vWF binding. A critical step in the processing is the proteolytic cleavage within the B-domain. This is typically performed by the protease furin (or similar proprotein convertases) at residues 1313 and 1648, resulting in the formation of the HC and LC heterodimer that is secreted into the plasma. In primary ECs, FVIII is co-stored with vWF in Weibel-Palade bodies. This co-storage is mediated by their interaction at the low pH (≈pH5.5) of the granules, ensuring that FVIII is released into the circulation already bound to its carrier protein (Haberichter and O'Donnell 2025; Kaufman et al., 1997).

2.2.2.3 Proteolytic cleavage and activation

The final activation of FVIII into its procoagulant form, FVIIIa, occurs at the site of injury. Thrombin cleaves FVIII at three specific sites: Arg372, Arg740 (within the HC), and Arg1689 (within the LC; Figure 3). The cleavage at Arg1689 is particularly important as it releases the a3 region, thereby triggering the dissociation of FVIIIa from vWF. (Fulcher et al., 1985; Banerjee et al., 2011). The resulting FVIIIa is a heterotrimer (consisting of the A1 subunit, the A2 subunit [HC], and the A3-C1-C2 [LC]). This heterotrimer is active but inherently unstable, as the A2 subunit is only weakly associated and spontaneously dissociates, leading to the rapid loss of cofactor activity, a key mechanism for limiting the duration of clot formation (Van Den Biggelaar et al., 2011; Mazurkiewicz-Pisarek et al., 2016)

2.3 The function of FVIII

As described, FVIII plays a major role in the non-enzymatic cofactor of the Xase complex, which is responsible for the activation of factor X and subsequent thrombin generation in secondary hemostasis (Mazurkiewicz-Pisarek et al., 2016; Fay, 2006). Deficiency or dysfunction of FVIII results in HA an inherited bleeding disorder whose associated comorbidities, including reduced bone mineral density and other extra-articular complications, go beyond what a coagulant role would predict (Graw et al., 2006; Mazurkiewicz-Pisarek et al., 2016). This has driven growing

interest in extra-coagulative, or extra-hemostatic, functions of FVIII that operate independently of its role in the Xase complex.

2.3.1 Hemophilia A

As described, HA is a congenital X-linked bleeding disorder resulting from mutations in the *F8* gene, leading to deficient or dysfunctional FVIII (Graw et al., 2005). The clinical phenotype is characterized by a tendency toward spontaneous and trauma-induced hemorrhage, particularly within the joints (hemarthrosis) and deep tissues (Graw et al., 2005; Klintman et al., 2013). In the absence of adequate FVIII activity, the secondary hemostatic response is severely compromised, resulting in prolonged bleeding and, historically, significant morbidity and mortality (Graw et al., 2005; Mazurkiewicz-Pisarek et al. 2016). Current therapeutic strategies focus on FVIII replacement or the use of bypassing agents to restore hemostatic balance (Klintman et al., 2013).

2.3.2 Extrahemostatic roles of FVIII

While its procoagulant function is well-defined, emerging research suggests that FVIII possesses extra-coagulative activities that influence bone metabolism, vascular stability, and immune modulation, highlighted by the co-morbidities related to HA (De Pablo-Moreno et al., 2022). These extra-hemostatic roles appear to involve direct interactions between FVIII and various cell surface receptors or ECM components, independent of its participation in the coagulation cascade (Cadè et al., 2022).

2.3.2.1 Endothelial cells

Endothelial cells represent a primary site of FVIII synthesis and regulated secretion (Rosenberg et al., 1998; De Pablo-Moreno et al., 2022). Within ECs, FVIII is co-packaged with vWF in Weibel-Palade bodies (Van Den Biggelaar et al., 2011; Rosenberg et al., 1998). Beyond its role as a reservoir for circulating FVIII, the endothelium relies on FVIII for maintaining vascular barrier integrity and promoting angiogenesis (Banerjee et al., 2011). Studies have indicated that FVIII activates the FAK/Src signalling pathway in ECs, which subsequently regulates the expression of Nidogen-2 (NID2), an ECM protein essential for basement membrane stability and endothelial migration (Olgasi et al., 2024). Consequently, FVIII deficiency has been associated with increased vessel permeability and impaired angiogenic responses (De Pablo-Moreno et al., 2022).

2.3.2.2 Bone

The association between FVIII and bone health is increasingly recognized, driven by the observation that HA patients exhibit a high prevalence of osteopenia and osteoporosis, often independent of joint bleeding history (Graw et al., 2005; Mazurkiewicz-Pisarek et al., 2016). Factor VIII appears to play a regulatory role in bone remodelling by influencing the balance between osteoblast and osteoclast activity. Preliminary evidence suggests that FVIII modulates the RANKL/OPG axis; specifically, FVIII deficiency may favor osteoclastogenesis and bone resorption, while its presence supports osteoblast differentiation and calcium deposition (Mazurkiewicz-Pisarek et al. 2016; Caliogna et al., 2025). This suggests that FVIII may function as a protective factor for bone mineral density, although the precise molecular mechanisms and the relative contribution of thrombin signalling require further elucidation.

2.3.2.3 Macrophage polarization

FVIII is also involved in the regulation of the immune landscape, especially regarding macrophage plasticity. Macrophages can assume different activation statuses from pro-inflammatory (M1) to anti-inflammatory and pro-tumor (M2; Mantovani and Locati, 2013). Macrophage polarization has been shown to be dependent on the presence of FVIII, as opposed to its absence. *In vitro* stimulation of patient-derived macrophages with the FVIII results in a pro-inflammatory M1 phenotype, while macrophages from patients receiving the non-FVIII based prophylactic Emicizumab are more resistant to M1 polarization but more prone to polarization toward an M2-like and Arg-1 high profile (Mantovani and Locati, 2013; Rhee, 2016; Boutilier and Elsawa, 2021; Cottonaro et al., 2026). The intersection of FVIII and macrophage biology is particularly relevant in the context of the tumor microenvironment, where tumor-associated macrophages (TAMs) frequently facilitate immune evasion and metastatic spread (Liu et al. 2021; Zhang et al. 2024; Yusupovna et al., 2025).

2.4 Evidence to support a role for FVIII in the pathophysiology of cancer

The recognition of FVIII as a potential player in cancer pathophysiology represents a significant shift from its traditional role in systemic hemostasis (Walker et al., 2022). This involvement is characterized by the ectopic expression of FVIII within malignant tissues, in particular neoplastic cells, and its direct contribution to tumor cell survival and progression (Walker et al., 2022).

2.4.1 Cancer cell FVIII production

One of the most important advances in the knowledge of FVIII in cancer was the observation that tumors themselves can express and produce FVIII directly. Walker *et al.* were the first to show that FVIII mRNA and protein are upregulated in bladder cancer compared to healthy matched tissue, and that FVIII is synthesized and secreted directly from bladder cancer cell lines (Walker et al., 2022). This was extended to show a broad expression of FVIII across a large profile of cancer types and stages, with FVIII protein expression specific to neoplastic cells, also seen in hepatocellular carcinoma (HCC) and oesophageal squamous cell carcinomas (ESCC) in another study (Mazurkiewicz-Pisarek et al., 2016; Walker et al., 2022). With a clear cellular localization to cancer cells identified by immunohistochemistry, the Cancer Cell Line Encyclopedia (CCLE) data base from the Broad Institute (https://portals.broadinstitute.org/ccle), FVIII mRNA, as well as other members of the coagulation cascade, was examined broadly in ≈800 cancer cell lines (16 tissue-of-origin groups). Factor VIII mRNA was shown to be significantly elevated in many cancer cell lines in an origin-dependent manner, with the highest expression seen in thyroid, lung, and pancreatic lines (Figure 4). Importantly, this elevated FVIII

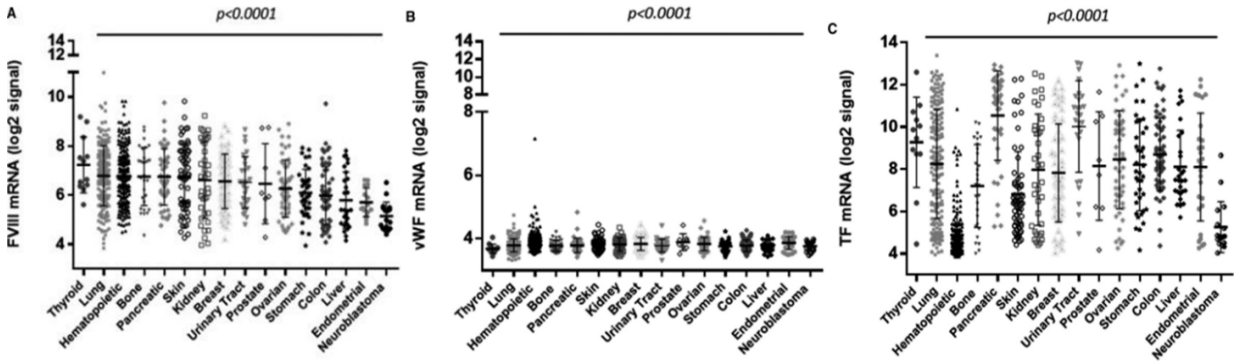


Figure 4: The relative expression levels (log2 signal) of FVIII, vWF, and TF mRNA across different human cancer cell lines *(Walker et al. 2022).*

mRNA pattern across cancer cell lines was found to be second only to TF expression, amongst the coagulation factors investigated (Walker et al., 2022). To confirm the cancer cell FVIII mRNA results extended to protein production, FVIII protein was studied by western blot in whole cell lysates and medium after 24hrs of culture. In 27 cell lines a differential secretion pattern was observed varying according to tumor type and grade, indicating that FVIII secretion and bioactivity is cell-type specific. Interestingly, the investigation of the secretion pattern identified in a broad array of cancer cell lines the strong presence of FL-FVIII; Figure 5) in thyroid, haematological, bone, breast and liver amongst others (Walker et al., 2022). This was unexpected given the processing of FL-FVIII prior to secretion as described in Section 2.2.2.2,

where secreted FVIII is thought to consist exclusively of HC+LC and intermediate processed forms. Such observations based on the structural and biosynthetic differences raised the possibility that FL-FVIII may have distinct biological activities in cancer compared with the more widely studied BDD-FVIII. Tumour-cell–derived FL-FVIII may engage signalling pathways or microenvironmental interactions that are not fully recapitulated by BDD-FVIII, providing a rationale for investigating FL-FVIII as a specific molecular species in cancer biology (Walker et al., 2022; Walker et al., 2025).

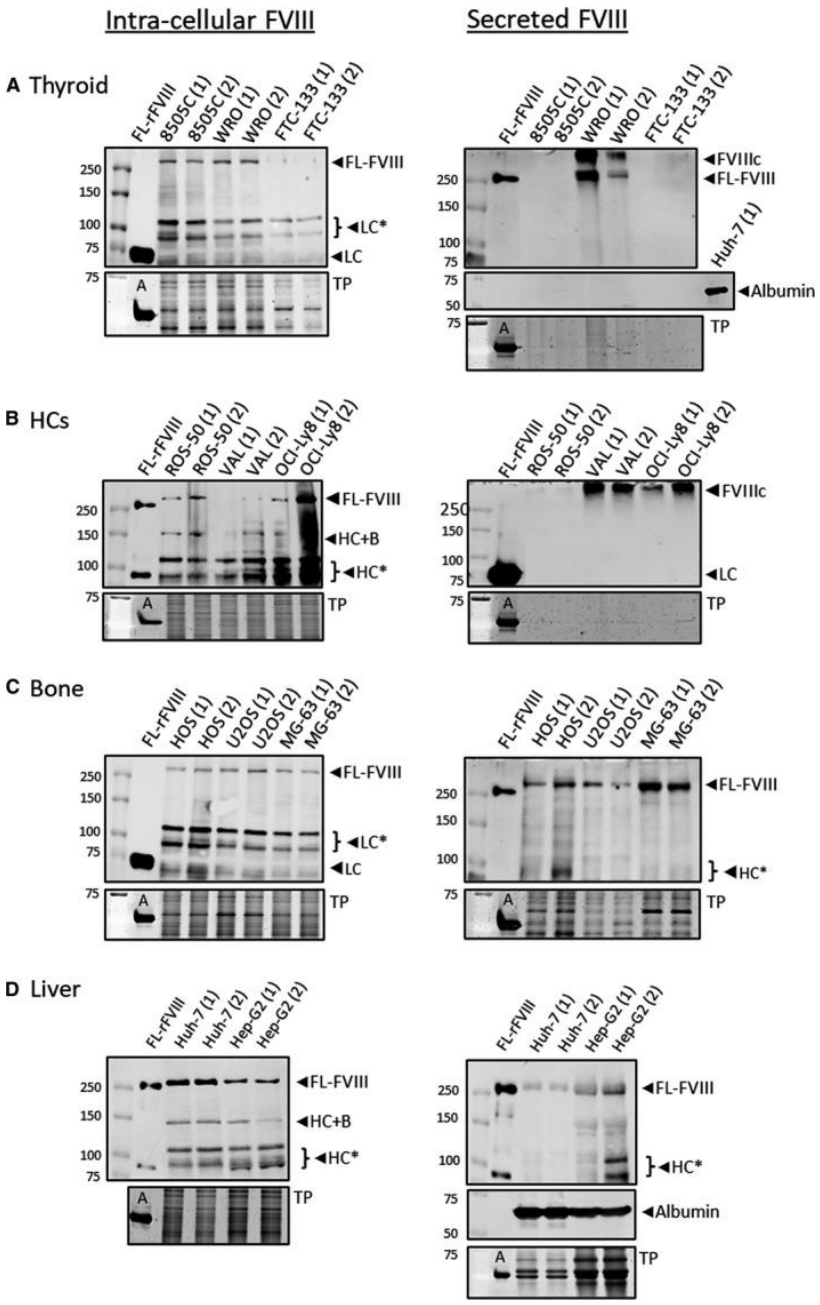


Figure 5: Detection of full-length FVIII (FL-FVIII) in cancer cell lines of diverse tissue origin. *(Walker et al. 2022)*

2.4.2 Direct effect of FL-FVIII

The effects of FL-FVIII on the behaviour of cancer cells has been illustrated in bladder cancer cell lines. Recombinant human FL-FVIII (rFL-FVIII) was found to promote the progression of cell cycle and the increase of migration in bladder cancer cell lines, with a significantly greater effect on rFL-FVIII compared to rBDD-FVIII (Walker et el., 2025). These effects on survival while seen in another unrelated cancer cell line (osteosarcoma U2OS), also showed rFL-FVIII increased levels of integrin β1 and αV (cell adhesion), decreased annexin-V/7-AAD positivity (apoptosis), maintained levels of Bcl2 (survival) and procaspase-3 (apoptosis), and maintained CREB signalling (Walker et el. 2025). These gain-of-function results were complemented by silencing of cancer cell–derived FVIII, which slowed down cell cycle progression and migration, and dramatically reduced cell survival. Administration of rFL-FVIII was able to completely rescue the phenotype (Walker et el. 2025). These findings highlighted FL-FVIII as a relevant survival factor in cancer cells, providing functional evidence for a role in cancer, outside of its canonical coagulant activity.

3. OBJECTIVE

The purpose of this Master's thesis, conducted in the Histology Laboratory of Professor Follenzi, is to assess whether FL-FVIII derived from cancer cells is directly involved in the malignant phenotype. This question is prompted by two converging lines of evidence: firstly, an unexpected observation that a broad array of cancer cells secretes FL-FVIII, and secondly, recombinant FL-FVIII (rFL-FVIII) has been demonstrated to be relevant survival factor in bladder and bone cancer models in low serum conditions. The experimental approach will be to create a stable cancer cell line producing FL-FVIII using lentiviral (LV) delivery. Given the indirect and direct regulation of FVIII by TF, two cell lines will be selected based on a low to negative FVIII production, and the expression or absence of TF. These cell models will be transduced with LV-FL-FVIII to generate cancer cell-derived production. Following the confirmation of production, the impact of cell-derived FL-FVIII will be examined on key oncogenic processes, including proliferation, migration, long-term survival, colony-forming capacity, the procoagulant phenotype through TF production, and an initial investigation into the molecular mechanisms co-involved. Overall, this study aims to determine whether stable expression of cancer-derived FVIII alters cancer cell behaviour to gain further insight into the potential extra-hemostatic role of FVIII in cancer progression.

4. MATERIAL AND METHODS

4.1 Cell culture and treatment

The human ovarian cancer cell lines A2780 (CVCL_0134), IGROV-1 (CVCL_1304), and SKOV3 (CVCL_0532) were maintained in Roswell Park Memorial Institute 1640 medium (RPMI-1640; EuroClone) supplemented with 10% fetal bovine serum (FBS; EuroClone) and 1% penicillin-streptomycin (P/S) and cultured at 37°C in a humidified atmosphere containing 5% CO_2. HUH7 (CVCL_0336) cells were maintained under the same conditions in Dulbecco's Modified Eagle Medium (DMEM) supplemented with 10% FBS and 1% P/S.

Functional assays were performed in 6- or 12-well plates, and whole-cell lysates were collected from cells cultured in 6-cm dishes. Cells were seeded in complete growth medium (10% FBS) and allowed to attach for 24 hours, after which the medium was replaced with 0.5% FBS for the duration of the assay. Seeding densities were as follows: 0.8×10^5 cells for proliferation assays, confluent monolayers for migration assays, 3×10^5 cells for survival assays, $1 \times$ or 3×10^3 cells for colony-forming assays, and 4×10^5 cells for whole-cell lysate preparation. All experiments were performed in a medium containing 0.5% FBS, with a minimum of three independent replicates.

4.2 Lentiviral (LV) transduction

Lentiviral vectors were produced in-house at the MOGM/P2 facility, approved by the Italian Ministry of Health, using the method of Follenzi and Naldini (Follenzi and Naldini, 2002). Viral titers were expressed as transducing units per millilitre (TU/mL). The FVIII-encoding LV transfer plasmid (hPGK-FVIII-FL-P2A-PuroR) is 14821 bp long (Figure 6A). It is third generation, self-activating LV vector with the human phosphoglycerate kinase (PGK) promoter was used for stable expression. The transgene comes from cDNA consisting of full length human FVIII (signal peptide-A1-A2-B Domain-A3-C1-C2). The P2A self-cleaving peptide sequence links FVIII in frame to puromycin resistant gene (PuroR) enabling selection of stably transduced cells. The vector includes a woodchuck hepatitis virus post-transcriptional regulatory element (WPRE) downstream of the insert to enhance transgene expression. The plasmid retains the HIV-1 packaging signal (ψ), Rev response element (RRE), and central polypurine tract (cPPT/CTS) to support efficient packaging and nuclear import. The control vector (LV-CTR; hPGK.P2A.PuroR, 6,492 bp) shares the same backbone and puromycin selection cassette but lacks the FVIII coding sequence (Figure 6B).

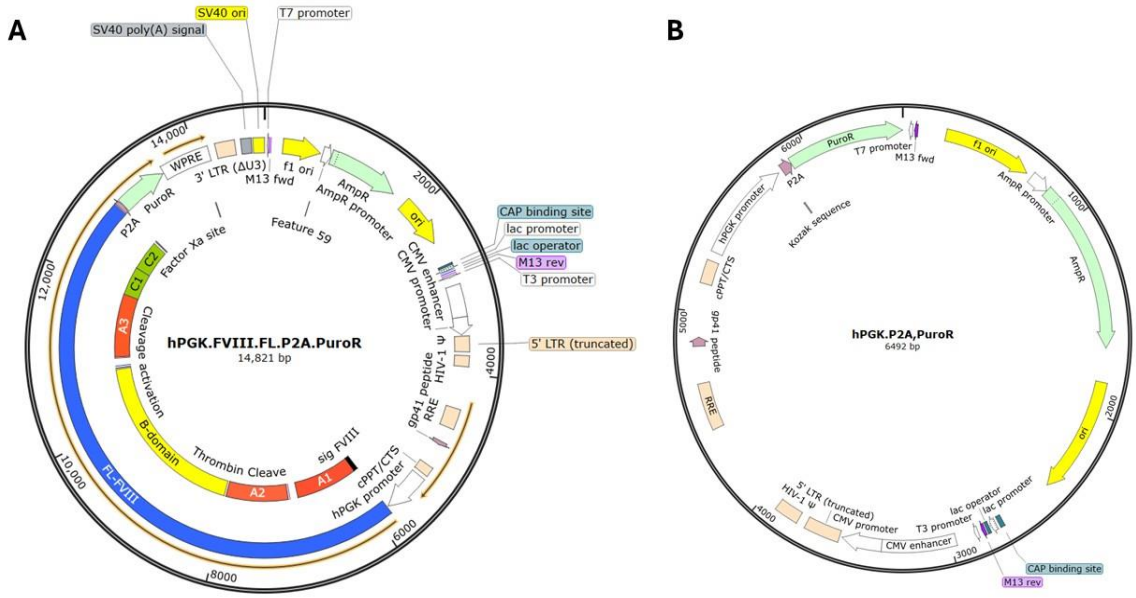


Figure 6: Lentiviral transfer vector maps. *(A) hPGK.FVIII.FL.P2A.PuroR (14,821 bp), encoding full-length FVIII linked to a puromycin resistance cassette via a P2A self-cleaving peptide. (B) hPGK.P2A.PuroR (6,492 bp), the corresponding empty control vector.*

To characterize transduction efficiency, candidate cancer cells were seeded at a density of 1.0 × 10^5 cells per well in 6-well plates 12–15 hours prior to transduction and subsequently transduced with a LV vector encoding green fluorescent protein under the phosphoglycerate kinase promoter (LV-PGK-GFP) at multiplicities of infection (MOI) of 1 and 5. Transduction efficiency was monitored over time by live-cell fluorescence microscopy (EVOS, Life Technologies) and quantified at 72 hours post-transduction by flow cytometry (FACS).

For functional studies, the selected cancer cells lines were seeded as described above and transduced with either a control vector (LV-CTR) or a vector encoding FVIII (LV-FVIII) at MOIs of 2, 5 and 10. Stably transduced populations were selected using puromycin (Sigma-Aldrich); this concentration was defined by a puromycin kill-curve titration (0.1–2.0 µg/mL) performed over 72 hours on the candidate cell lines, identifying the minimum concentration required to achieve complete cell death.

4.3 Quantification of transduction efficiency by FACS

At 72 hours post-transduction, LV-PGK-GFP-transduced cells were harvested with trypsin-EDTA, centrifuged (1,100 rpm, 5 min, room temperature), and washed twice in 1× phosphate-

buffered saline (PBS). Cells were then resuspended in 500 µL FACS buffer (1× PBS, 5% FBS, 2 mM EDTA), and GFP expression was quantified by flow cytometry (Attune, Thermo Fisher Scientific). Data were analyzed using FlowJo software (v10; Becton Dickinson) and expressed as the percentage of GFP-positive and GFP-negative cells.

4.4 Integrated Vector copy number (VCN) analysis

Vector copy number (VCN) for each MOI was determined for LV-FVIII-transduced populations. Genomic DNA was extracted from transduced cells using the Tissue DNA Purification Kit (Promega) and quantified using nanodrop. Conventional PCR was used to verify primer specificity and expected amplicon size prior to quantitative analysis, PCR was performed using GoTaq Flexi DNA Polymerase (Promega)**,** 28 cycles (25 cycles for GAPDH) of denaturation at 95°C for 30 seconds, annealing at 60°C for 30 seconds, and extension at 72°C for 40 seconds, with a final extension at 72°C for 7 minutes. PCR products were resolved on 2% agarose gels. The VCN integrated was then assessed by quantitative PCR using a primer pair spanning the hPGK promoter and the FVIII coding sequence (forward, PGK: 5′-GTTCCGCATTCTGCAAGTC-3′; reverse, FVIII A2: 5′-AGAAGCAGGTGGAGAGCTC-3′) and a primer pair targeting the single-copy reference gene GAPDH (forward: 5′-AGTGGGTGTCGCTGTTGAAGT-3′; reverse: 5′-AACGTGTCAGTGGTGGACCTG-3′). Standard curves were generated separately for the FL-FVIII and GAPDH amplicons: the FL FVIII standard curve used serial dilutions of the transfer vector plasmid, and the GAPDH standard curve used serial dilutions of genomic DNA from the corresponding cell line, starting at 33 ng/µL; absolute copy numbers were interpolated from the corresponding curve for each target. The number of integrated proviral copies per cell was calculated as the ratio of FL-FVIII copies to GAPDH copies (normalized per diploid genome), confirming accurate delivery of the intended MOI prior to downstream functional and molecular experiments. Values are expressed as integrated copies/diploid genome.

4.5 RNA extraction and RT-qPCR analysis of FVIII expression

Total RNA was extracted from cancer cells grown to confluency, using Isol-RNA Lysis Reagent (Invitrogen) according to the manufacturer's instructions. Cells were lysed directly in the reagent, and phase separation was achieved by the addition of chloroform followed by centrifugation. The aqueous phase containing RNA was precipitated with isopropanol, washed with 75% ethanol, and resuspended in RNase-free water. RNA concentration and purity (A260/A280 ratio) were assessed spectrophotometrically using NanoDrop (ThermoFisher Scientific)

One microgram of total RNA was treated with DNase I (Invitrogen) to eliminate genomic DNA, and complementary DNA (cDNA) was synthesized using the RevertAid First Strand cDNA Synthesis Kit (Thermo Fisher Scientific), according to the manufacturer's instructions.

Conventional end-point PCR was used to verify primer specificity and expected amplicon size prior to quantitative analysis, PCR was performed using GoTaq Flexi DNA Polymerase (Promega), with an initial denaturation at 95°C for 5 minutes, followed by 28 cycles (25 cycles for β-actin) of denaturation at 95°C for 30 seconds, annealing at 60°C for 30 seconds, and extension at 72°C for 40 seconds, with a final extension at 72°C for 7 minutes. PCR products were resolved on 2% agarose gels.

Quantitative real-time PCR. RT-qPCR was performed to evaluate FVIII transgene expression using a primer pair spanning the FVIII–PuroR junction of the lentiviral construct (forward, targeting the FVIII C2 domain: 5′-AGTTCCTCATCTCCAGCAGTC-3′; reverse, targeting the puromycin resistance sequence: 5′-GGAAGAGTTCTTGCAGCTCG-3′), designed to specifically detect the transgene-derived transcript. Reactions were carried out in 20 µL volumes containing SYBR Green PCR master mix (Thermo Fisher Scientific) and cDNA diluted 1:10, on a StepOnePlus Real-Time PCR System (Applied Biosystems). Cycling conditions consisted of an initial denaturation step at 95°C for 10 minutes, followed by 40 cycles of denaturation at 95°C for 15 seconds and combined annealing/extension at 60°C for 1 minute. β-Actin was used for normalization of target gene expression, and relative FVIII mRNA expression was calculated using the comparative 2^−ΔΔCt method (Livak and Schmittgen, 2001), with data expressed as fold change relative to the appropriate control. Reactions were performed in duplicate across 3 independent experiments.

4.6 Live-cell imaging for proliferation and survival

Live-cell imaging for proliferation and survival assays was performed using an IncuCyte SX5 system (Sartorius). For proliferation assays, images were acquired every 6 hours over a 72-hour period. For survival assays, cells were stained with TO-PRO-3 (1 µM) at the end of day 6 post-seeding and imaged every 6 hours over the following 24 hours. At assay completion, cell-by-cell analysis of adherent cells was performed using IncuCyte software. Two independent experiments were performed in triplicate.

4.7 Colony-forming assay (CFA)

Colony formation was monitored daily for >14-day period using an inverted microscope (Leica DMi1, Leica Microsystem). At the assay endpoint, colonies were fixed and stained with 0.5% crystal violet (w/v in 20% methanol), and representative images were acquired using a ChemiDoc Touch Imaging System (Bio-Rad). Image analysis was performed in Fiji (ImageJ, National Institutes of Health). Colony counts were calculated on pixel intensity (total stained area per well). Total stained area was recorded for each well and expressed relative to the corresponding LV-CTR condition within each independent experiment (colony formation, % of LV-CTR = stained area in treated well / stained area in LV-CTR well × 100), to account for inter-experimental variation in plating efficiency. Data are reported from n=3 independent experiments.

4.8 Migration Assay

Cells were seeded in 12-well plates and allowed to reach confluency. A cross-shaped scratch was made across each well, and cells were then maintained in 0.5% FBS medium. Migration was monitored by phase-contrast imaging using an inverted microscope (Leica DMi1, Leica Microsystem) at 0 (T0), 6, 9, and 24 hours post-scratch. Percentage wound closure relative to T0 was quantified using ImageJ software (National Institutes of Health).

4.9 Protein extraction and western blot analysis

Whole-cell lysates from cancer cells were prepared by mechanical disruption in RIPA buffer (50 mM Tris-HCl pH 7.5, 150 mM NaCl, 1% NP-40, 1% sodium deoxycholate, 0.1% SDS) supplemented with 1× EDTA-free protease (Merck) and phosphatase inhibitors. Protein concentration was determined using the Pierce BCA Protein Assay (Thermo Fisher Scientific). Samples (10 µg per lane) were resolved by SDS-PAGE (7.5%, 10%, or 15% gels) under reducing conditions and transferred to polyvinylidene difluoride (PVDF) membranes (Bio-Rad). Membranes were probed with primary antibodies against Integrin β1 (1:4000; Cell Signaling Technology), Integrin β3 (1:3000; Cell Signaling Technology), Integrin α6 (1:3000; Cell Signaling Technology), Integrin α5 (1:3000; Cell Signaling Technology), Integrin αV (1:3000; Cell Signaling Technology), phospho-FAK (1:2000, Cell Signaling Technology), FAK (1:3000, Cell Signaling Technology), phospho-Src (1:2000; Cell Signaling Technology), Src (1:3000; Cell Signaling Technology), TF (1:3000; Cell Signaling Technology), phospho-IRE1 (1:2000; Cell Signaling Technology), IRE1 (1:2000; Cell Signaling Technology), phospho-eIF2α (1:2000; Cell Signaling Technology), eIF2α (1:2000; Cell Signaling Technology), Caspase 12

(1:2000; Abcam), ProCaspase3 (1:3000; Abcam), NRF1 (1:2000; SantaCruz), BCL2 (1:3000; Cell Signalling Technology) and CHOP (1:1000; Santa Cruz). Either polyclonal anti-FVIII-HRP antibody (1:10000, Thermo Fischer Scientific) or monoclonal anti-FVIII-C2 antibody (1:10000; Green Mountain) was used to detect FL-FVIII. Excluding anti-FVIII-HRP, all antibodies were detected with horseradish peroxidase (HRP)-conjugated secondary anti-rabbit or anti-mouse antibodies (1:5000; Merck). A monoclonal β-Actin-HRP, 1:20,000; Merck) served as the loading control for normalization. Immunoreactive bands were visualized by enhanced chemiluminescence and imaged using a ChemiDoc Touch Imaging System (Bio-Rad).

4.10 Statistical analysis

Data are presented as mean ± standard deviation (SD). Depending on the experimental design, statistical significance was assessed by one- or two-way analysis of variance (ANOVA) with Tukey's post hoc test for multiple comparisons, or by Student's *t*-test, using GraphPad Prism software (version 8.0.1; GraphPad Software). A P-value < 0.05 was considered statistically significant.

5. RESULTS

5.1 Cancer cell lines selection and characterization to investigate the function of cell-derived FL-FVIII

To select an optimal panel of cancer cell lines to investigate the effect of FL-FVIII production, an assessment was made of FVIII and TF mRNA expression in cell lines according to tissue origin, and FL-FVIII secretion profiles from previously published data (Walker et al. 2022). The criteria for selection were: 1) low origin-specific FVIII mRNA expression; 2) the availability in-house of at least 3 cancer cell lines of the same tissue origin; 3) a very low to undetectable FL-FVIII secretion; and 4) TF mRNA expression levels for each cell line.

5.1.1 Ovarian cancer cell lines selected to study the effect of FVIII-FL production

According to the data available form Cancer Cell line Encyclopedia (CCLE) database (https://portals.broadinstitute.org/ccle) of mRNA expression (log2 signal), cancer origins with lowest FVIII mRNA expression profile were neuroblastoma (4.9±0.6), endometrial (5.7±0.6), liver (5.8±1.1), colon (6.0±1.2), stomach (6.1±1) and ovarian (6.1±1.2; Walker et al. 2022). Expression <5.5 log2signal was considered as negative expression. Of these, 3 cell lines were available in-house for colon (SW480, SW837, RKO) and ovarian cancer (A2780, IGROV1, SKOV3). An examination of the cell line specific FVIII and TF mRNA expression identified a lower FVIII mRNA expression in the 3 ovarian cell lines, with a variable TF mRNA expression (Table 1).

TABLE1: ***The mRNA expression (log2 signal) of FVIII and TF in selected colon and ovarian cancer cell lines from CCLE database.***

Cell Lines	FVIII mRNA (log2 signal)	TF mRNA (log2 signal)
COLON		
SW480	7.45	8.26
SW837	9.72	9.52
RKO	7.02	5.12
OVARIAN		
A2780	4.91	4.51
IGROV1	4.92	10.54
SKOV3	5.3	11.93

*Text highlighted in red low/negative expression

On the basis of FVIII expression, the panel of ovarian cancer cell lines (A2780, IGROV1, SKOV3), were selected to assess the cell-derived FVIII secretion. Serum-free medium collected after 72hr of culture was analysed by western blot using anti-FVIII-C2 antibody specific to the C-terminus of FVIII (Figure.7). A 72hr serum-free medium from HUH7, a hepatocellular carcinoma cell line, was used as a positive cell-derived FVIII control as it has previously been shown to secrete high levels of FL-FVIII (Walker et al., 2022). The A2780 and IGROV1 cells showed no evidence of FL-FVIII, however, they showed low secretion levels of the FVIII light chain (LC) and light chain + B-domain (LC+B), while SKOV3 showed no detectable secretion. Based on the secretion profile, all the ovarian cancer cell lines were considered suitable for subsequent experimentation aimed at assessing the function of FL-FVIII.

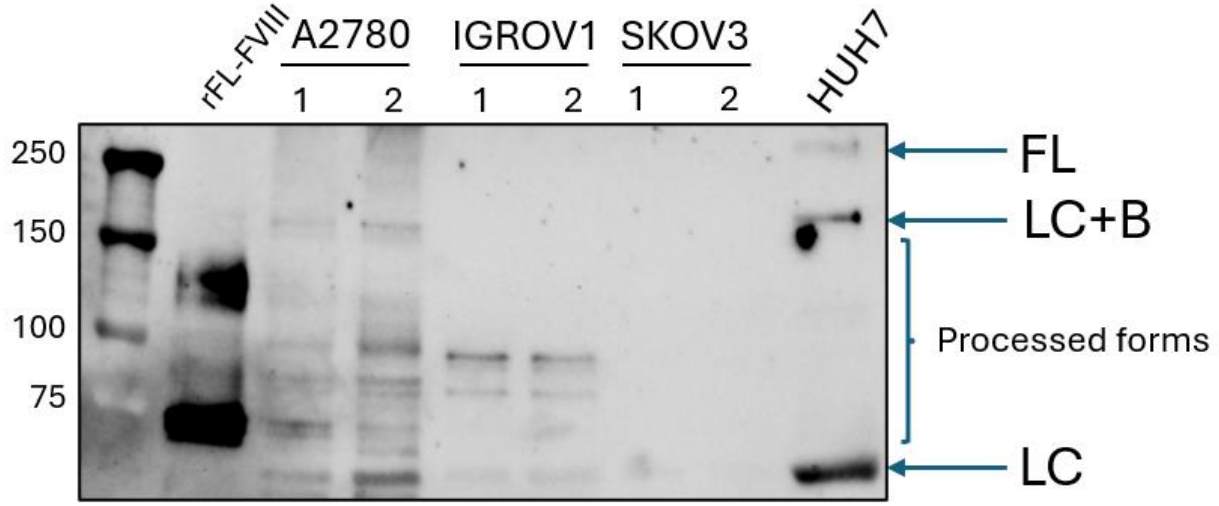


Figure 7: FVIII secretion in ovarian cancer cell lines. *Western immunoblot analysis of two independent conditioned serum-free media samples (1, 2), collected after 72hrs from A2780, IGROV1, and SKOV3. HUH7 conditioned media was used as a positive control for cell-derived FVIII while a recombinant FL-FVIII (rFL-FVIII) was run as a reference for FVIII band size. Arrows indicate the full-length (FL), light chain plus B-domain (LC+B), and light chain (LC) forms of FVIII, as well as intermediary processed forms.*

5.1.2 Establishing the lentiviral transduction efficiency in A2780, IGROV1 and SKOV3 cells using LV-PGK-GFP

Aiming to introduce to the ovarian cell lines a vector containing FL-FVIII driven by the PGK promoter with a puromycin resistance cassette (PGK-FL-FVIII-2APURO; refer to Figure 6 in the Materials and Methods), a LV delivery method was selected which allows for integration into the genome. This requires an assessment of transduction efficiency for each cell line using LV-PGK-GFP with increasing MOI (MOI1 and 5). For A2780 cells this has previously been

established, with 52.6% GFP-positive cells for MOI1 and 88.1% for an MOI5 (MSc thesis, MG Melese, 2025).

A. **B.**

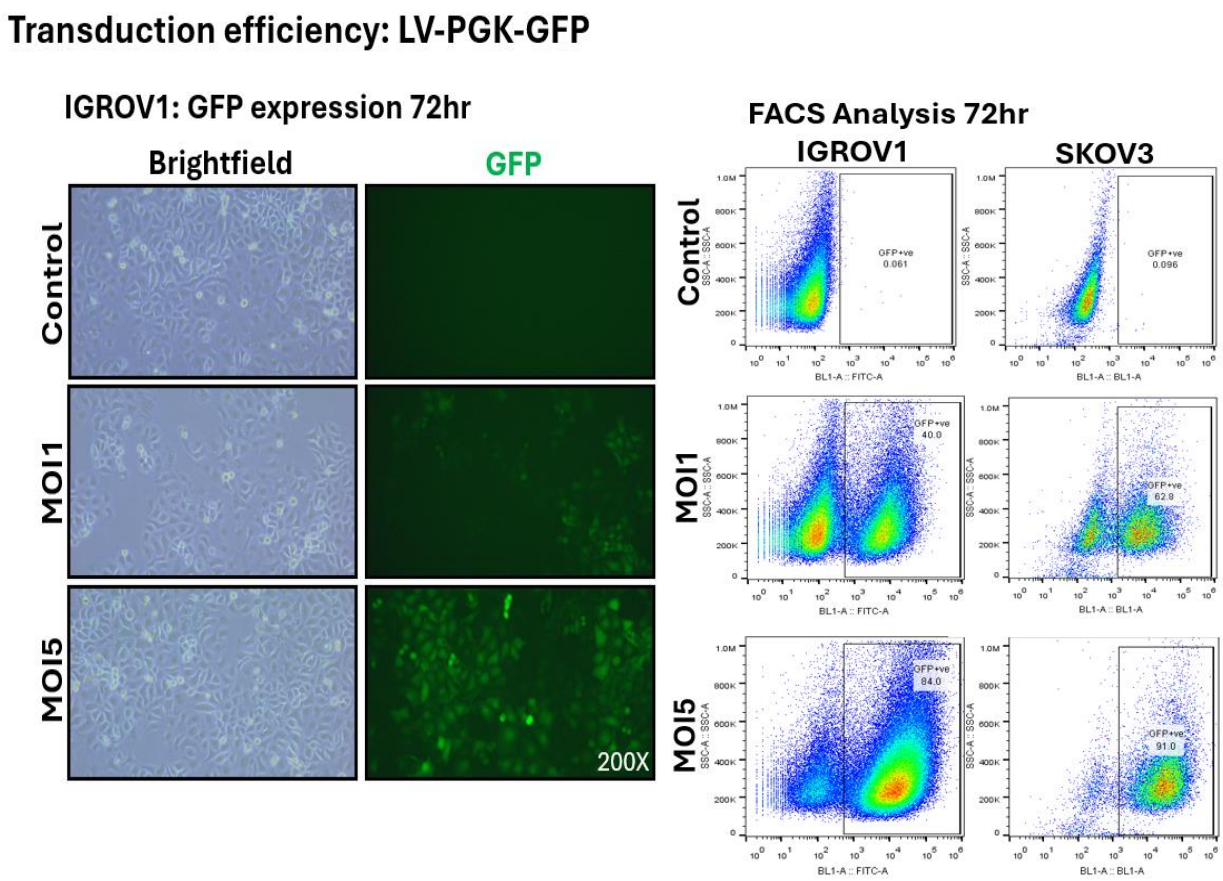


Figure 8: Optimization of LV transduction efficiency in IGROV1 and SKOV3 cells using LV-PGK-GFP. *(A) Representative images of PGK-GFP expression in IGROV1 at an MOI1 and MOI5 over 72hrs with live cell EVOS microscope. Magnification, 200X. (B) FACS analysis of GFP-positive cells in IGROV1 and SKOV3 at MOI 1 and MOI 5, alongside a non-transduced control (CTR). Percentages indicate the proportion of GFP-positive cells within each gated population, assessed 72hrs post-transduction.*

To determine the transduction efficiency of the two additional ovarian lines, IGROV-1 and SKOV3 were transduced with LV-PGK-GFP at an MOI of 1 and 5. At 72hrs post-transduction, cell viability and GFP expression were confirmed for both cell lines by live-cell fluorescence microscopy, providing initial evidence of successful transduction and preserved cell viability (Figure 8A). The GFP expression at 72hrs was quantified by FACS, where for IGROV1 40.0% of cells were GFP-positive at MOI 1, and 84.0% at MOI 5, while for SKOV3 GFP-positive cells were 62.8% at MOI 1 and 91.0% at MOI 5 (Figure 8B). These results confirmed a dose-dependent increase in transduction efficiency with increasing MOI inferring that both cell lines

could be efficiently transduced with lentiviral particles, supporting their use for subsequent transduction with the PGK-FVIII-FL-2APURO construct.

5.1.3 Optimization of puromycin selection for stable transduction

As the vectors carry a puromycin resistance cassette, the optimal puromycin concentration for selection was determined using a concentration gradient ranging from 0.1–2 µg/mL for IGROV1 and 0.1–3 µg/mL for SKOV3. Cell viability was visually monitored by brightfield microscopy over 72hrs, based on cell detachment and rounding, revealing a dose-dependent decline in viability with increasing puromycin concentration (Figure 9). A concentration of 1 µg/mL was identified as the minimum concentration for cell death of non-transduced cells for both IGROV1 and SKOV3, to be used for selection in all subsequent experiments. Puromycin selection for A2780 had been previously established at 0.5 µg/mL (MSc thesis, MG Melese, 2025) and was adopted for this work.

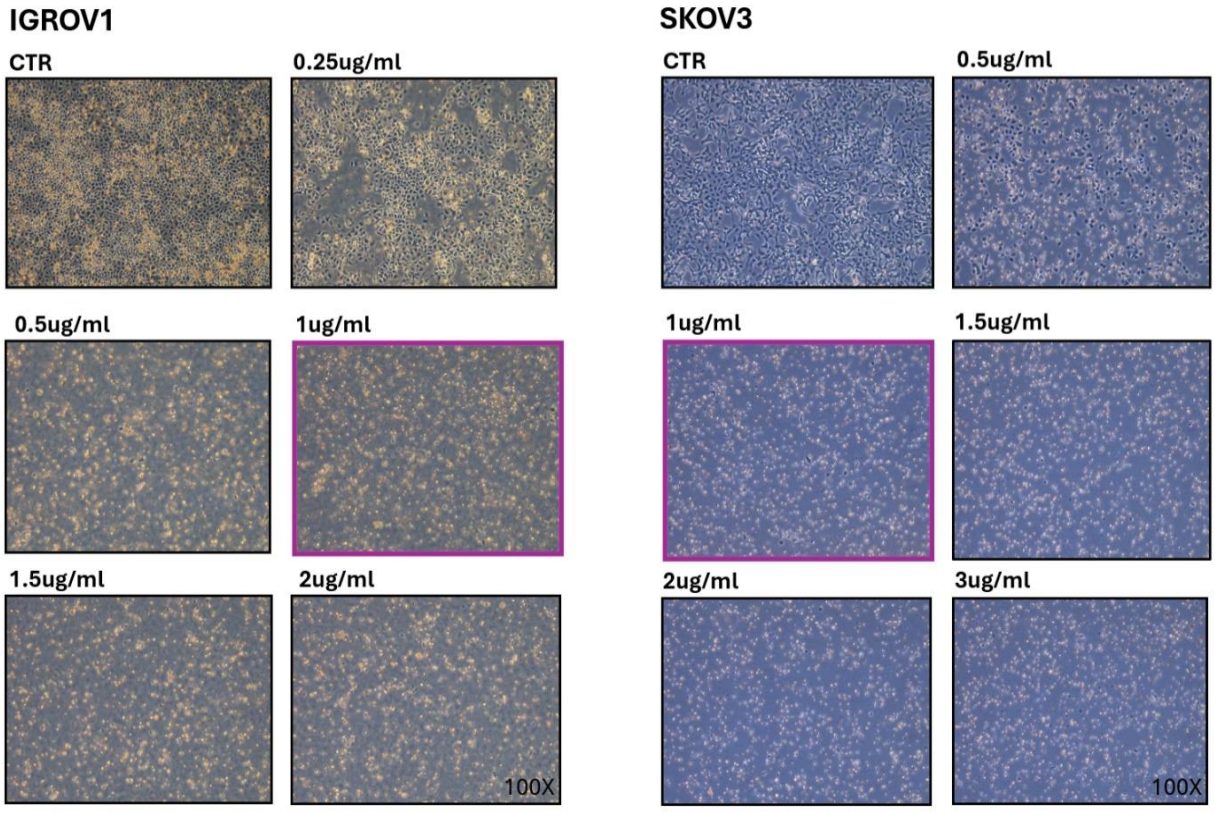


Figure 9: Optimization of the puromycin concentration required for selection in IGROV1 and SKOV3 cells. *Representative brightfield images of IGROV1 and SKOV3 cells treated with increasing concentrations of puromycin for 72 hrs. 100× magnification.*

5.2 Generation and validation of the ovarian cancer cells producing FVIII

Due to the long-term management of transduced cell lines, only the first two cell lines A2780 and IGROV1, each with a low FVIII expression but with a differential TF expression, were selected for an initial experimentation.

5.2.1 Generation of A2780 and IGROV1 cells producing cell-derived FL-FVIII

To generate cells expressing and secreting FL-FVIII, A2780 and IGROV-1 cells were transduced with control (LV-CTR) or FL-FVIII (LV-FVIII-FL) lentivirus at an MOI of 2, 5, and 10. At 72hrs post-transduction, puromycin selection was performed at 0.5 (A2780) or 1 µg/mL (IGROV1). With selection the non-transduced cells were eliminated and the viable cells expanded whereas cells suggesting a successful integration (Figure 10). To verify the integration a of FL-FVIII and its production by the cells, three complementary approaches were used: 1) quantification of vector copy number (VCN); 2) mRNA expression; and 3) an assessment of FVIII secretion into serum-free medium by western blot.

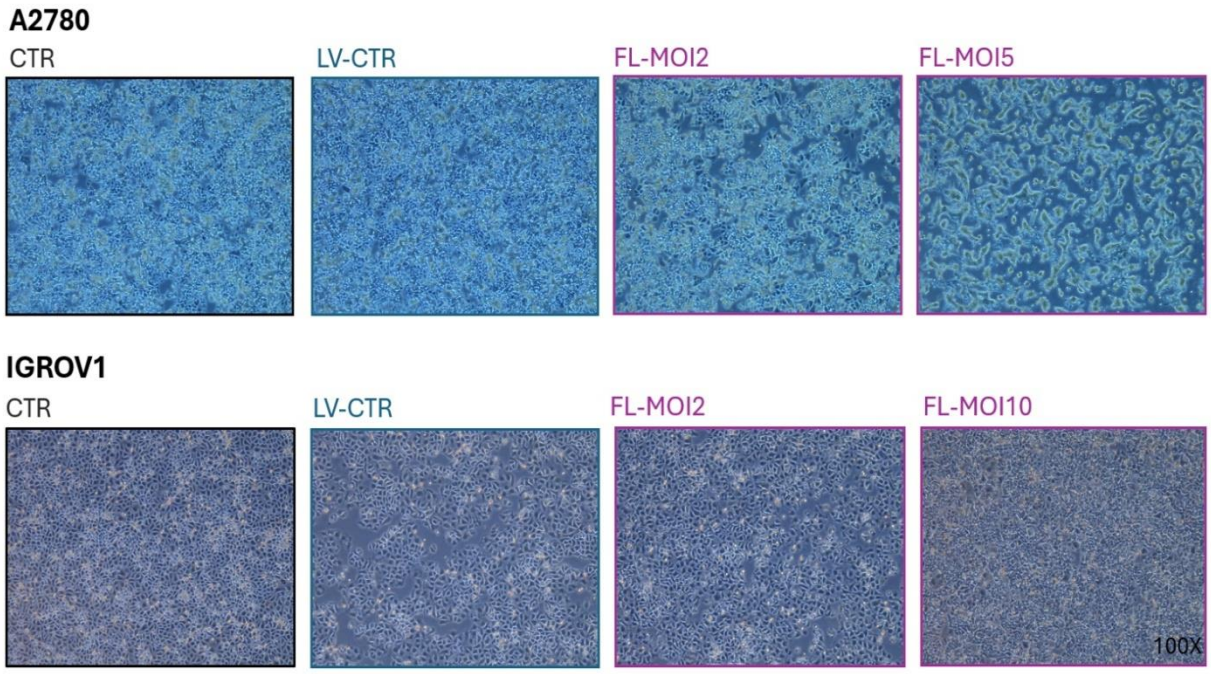


Figure 10: A2780 and IGROV1 cells following transduction, selection and expansion. *Representative bright-field images of control (CTR), cells transduced with control lentivirus LV-CTR-2APURO (LV-CTR), and cells transduced with LV-FVIII-2APURO MOI2 (FL-MOI2) and MOI 5(FL-MOI5). Images were taken 72hrs in serum-free media. Magnification, 100X.*

5.2.1.2 Vector copy number confirms dose-dependent lentiviral integration

To confirm vector integration, vector copy number (VCN) was determined by qPCR for A2780 and IGROV1 cells transduced with LV-FVIII-FL at increasing MOIs. In A2780 cells, VCN increased from 2.39 copies/diploid genome at MOI 2 to 7.43 at MOI 5. In IGROV1 cells, VCN increased from 1.5 copies/diploid genome at MOI 2 to 4.05 at MOI 10 (Figure 11). Non-transduced control cells showed near-zero VCN in both cell lines (A2780: 0.03; IGROV1: 0.08), consistent with residual background signal rather than true integration. These results confirm the integration of FL-FVIII in both cell lines, with copy number variably increasing at the higher MOI between the two cell lines.

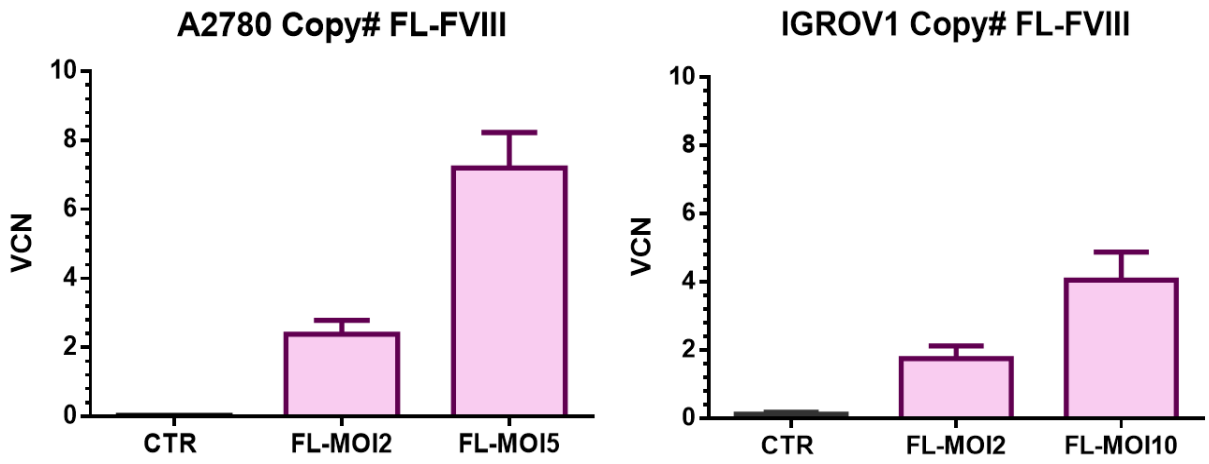


Figure 11: Vector copy number confirms dose-dependent integration. *Vector copy number (VCN) was determined by qPCR in A2780 and IGROV1 cells transduced with LV-FVIII-FL at increasing MOIs, alongside non-transduced controls (CTR). VCN increased in a dose-dependent manner in both cell lines. Data are expressed as mean integrated copies/diploid genome ± SD from n=3 repeats.*

5.2.1.2 The FVIII mRNA highlights a variable expression unrelated to VCN

The FVIII mRNA expression was assessed by RT-PCR in A2780 and IGROV1 cells transduced with LV-FVIII-FL, using a primer pair spanning the FL-FVIII coding sequence and P2A-PuroR junction (447 bp amplicon), with GAPDH (250 bp) as the control. No amplification was present in non-transduced (CTR) or LV-CTR control cells for both cell lines (Figure 12). Surprisingly, despite several repeats of the experiment, for the A2780 FL-FVIII cells only a faint FVIII mRNA expression could be detected at both MOIs, with a higher expression for FL-MOI2, with respect to FL-MOI10. This was also seen for the IGROV1 FL-FVIII cells, where a strong FVIII mRNA signal was detected at MOI 2, which decreased at MOI 10. A decreased FL-FVIII mRNA

expression seen for both cell lines at the higher vector copy number, highlights a transcriptional repression related to the vector size and/or the cellular metabolic health.

A.



B.

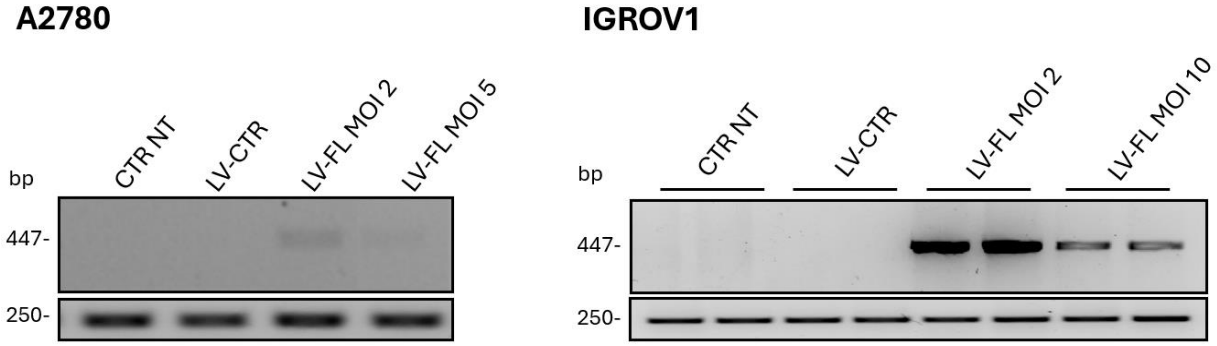


Figure 12: FL-FVIII mRNA expression from transduced A2780 and IGROV1 cells. *(A) Schematic showing the primer pair spanning the FVIII-FL coding sequence and P2A-PuroR junction, amplifying a 447bp product. (B) Agarose gel images of RT-PCR products from A2780 and IGROV1 CTR, LV-CTR, LV-FL MOI2 and MOI5 cells, with GAPDH (250bp) as the control.*

5.2.1.3 An inverse FVIII secretion pattern to VCN for FL-FVIII expressing ovarian cancer cells

To establish the production of FL-FVIII from A2780 and IGROV1 cells, secreted FVIII was analyzed by western blot in 72hr conditioned serum-free media using either the anti-FVIII-C2 antibody targeted to the C-terminus (A2780), or a polyclonal FVIII-HRP conjugated antibody (IGROV1; Figure 13). For the A2780 cells, a band corresponding to the light chain plus B-domain (LC+B) increased in the FL-MOI2 (VCN≈2copies) cells with respect to the controls (CTR, LV-CTR) yet decreased for the higher MOI (MOI5: VCN≈6copies) paralleling the mRNA results (Section 5.2.1.2). A similar pattern was also observed for the IGROV1 cells, with a band corresponding to the heavy chain (HC) of FVIII increasing in FL-MOI2 (VCN≈2copies) cells, while decreasing in FL-MOI10 (VCN≈4copies) cells. SyproRuby total protein stain confirmed that the differences were unrelated to the levels of secreted protein and thus protein production. Collectively, these results suggest there is a modest increase in FL-FVIII secretion with a

VCN≈2copies, while and impairment in FL-FVIII production is evident at the higher VCNs likely due to overloading.

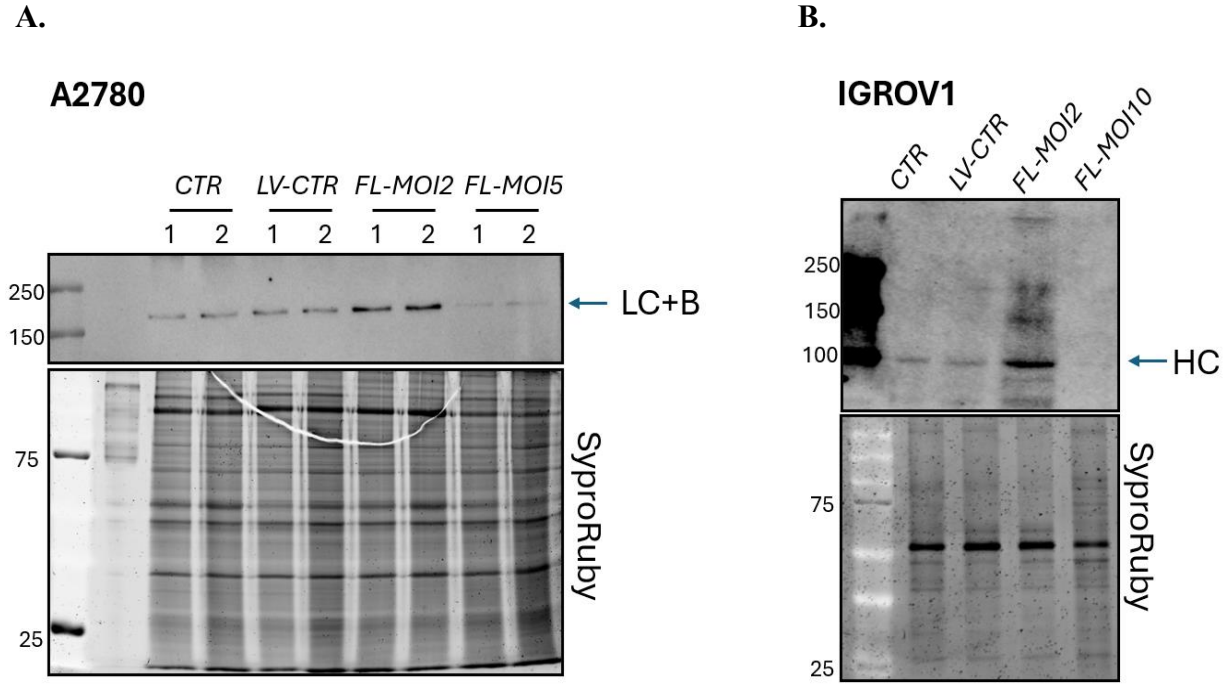


Figure 13: FVIII secretion pattern in from A2780 and IGROV1 FL-FVIII producing cells. *(A) Western immunoblot analysis of FVIII detecting the light chain plus B-domain (LC+B), and Sypro Ruby total protein staining of 72hr conditioned serum-free media from A2780 CTR, LV-CTR, and LV-FVIII-FL MOI2 (FLMOI2) and FLMOI5 cells of FVIII. (B) Western immunoblot analysis of FVIII detecting the heavy chain (HC) and Sypro ruby total protein staining of 72hr conditioned serum-free media from IGROV1 CTR, LV-CTR, and LV-FVIII-FL MOI2 (FL-MOI2) and FL-MOI5 cells of FVIII.*

5.3 Pathophysiological assessment of FL-FVIII producing A2780 and IGROV1 cells

Based on the molecular characterization of FL-FVIII producing ovarian cancer cells (Section 5.2.1), focus was given specifically to those cells with VCN≈2 (FL-MOI2) where a modest increase FL-FVIII production was evident. To assess the effect of cell-derived FVIII-FL on the pathophysiology of ovarian cancer cells, proliferation, migration and survival were evaluated in low serum conditions (0.5%FBS), aiming to represent more closely the tumour cell microenvironment. The A2780 and IGROV1 cells with a VCN>4 were included the proliferation experiments to provide for evidence to support a suspected metabolic overloading.

5.3.1 Proliferation is not influenced by an increase is cell-derived FL-FVIII production, while metabolic overloading has a negative impact.

The proliferation of A2780 and IGROV1 cells (CTR, LV-CTR, FL-MOI2, FL-MOI5 or 10) cultured in 0.5% FBS were monitored by live-cell imaging every 6hrs over a 24hr period. For

both A2780 and IGROV1, CTR, LV-CTR, and FL-MOI2 cells proliferated similarly with an increase in % growth with respect to T0 (Figure14). In contrast, A2780 and IGROV1 cells with a VCN>4 proliferated more slowly showing a showing a significantly slower growth as early as 12hr (Figure14). Collectively, the data highlights that an increase in cell-derived FL-FVIII has no effect on ovarian cancer cell proliferation, while for cells with a higher VCN, proliferation is significantly decreased, supporting the concept of metabolic overloading.

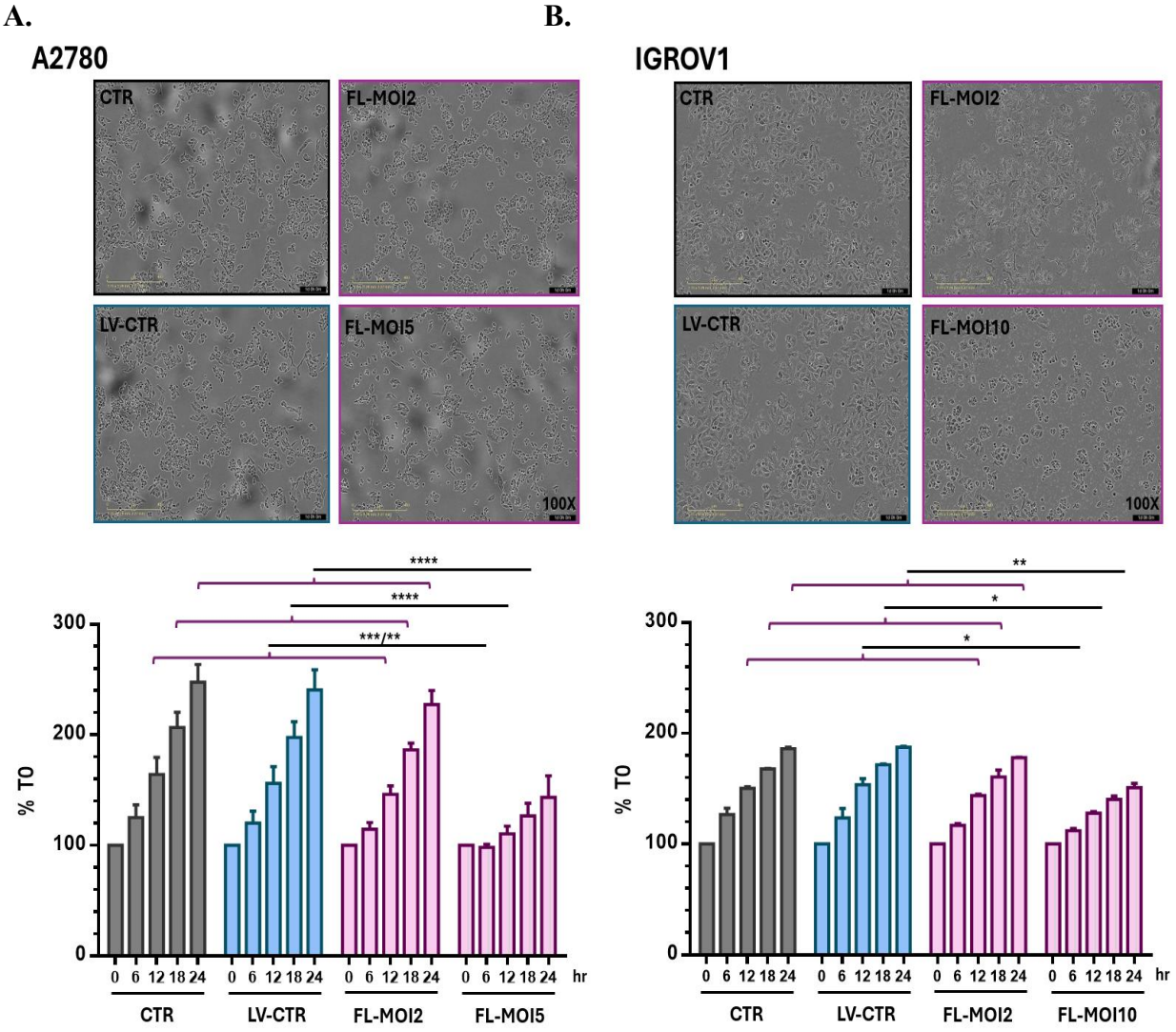


Figure 14: Cell-derived FL-FVIII has no impact on the proliferation of A2780 and IGROV1 cells. *(A) Representative bright-field images (magnification, 100X) at 24hrs and graphical representation of A2780 cellular proliferation over 24hrs in 0.5% FBS. (B) Representative bright-field images (magnification, 100X) at 24hrs and graphical representation of IGROV1 cellular proliferation over 24hrs in 0.5% FBS.*

5.3.2 Migration is not influenced by an increase in cell-derived FL-FVIII production

The migratory ability of A2780 and IGROV1 cells (CTR, LV-CTR, FL-MOI2) cultured in 0.5% FBS were assessed by a wound healing assay over a 24hr period, with images taken at T0, 6hr, 8hr and 24hr (n=5). The higher VCN lines for both cell lines were not assessed due to their inability to reach confluency in an appropriate time frame. In A2780 cells, the control (CTR, LV-CTR) and FL-MOI2 cells wounds closed in a comparable fashion by 24 hrs (~38%; Figure 15A), with similar results observed for IGROV1 (Figure XB). Together these results show that migration is not altered by an increase in cell-derived FL-FVIII production.

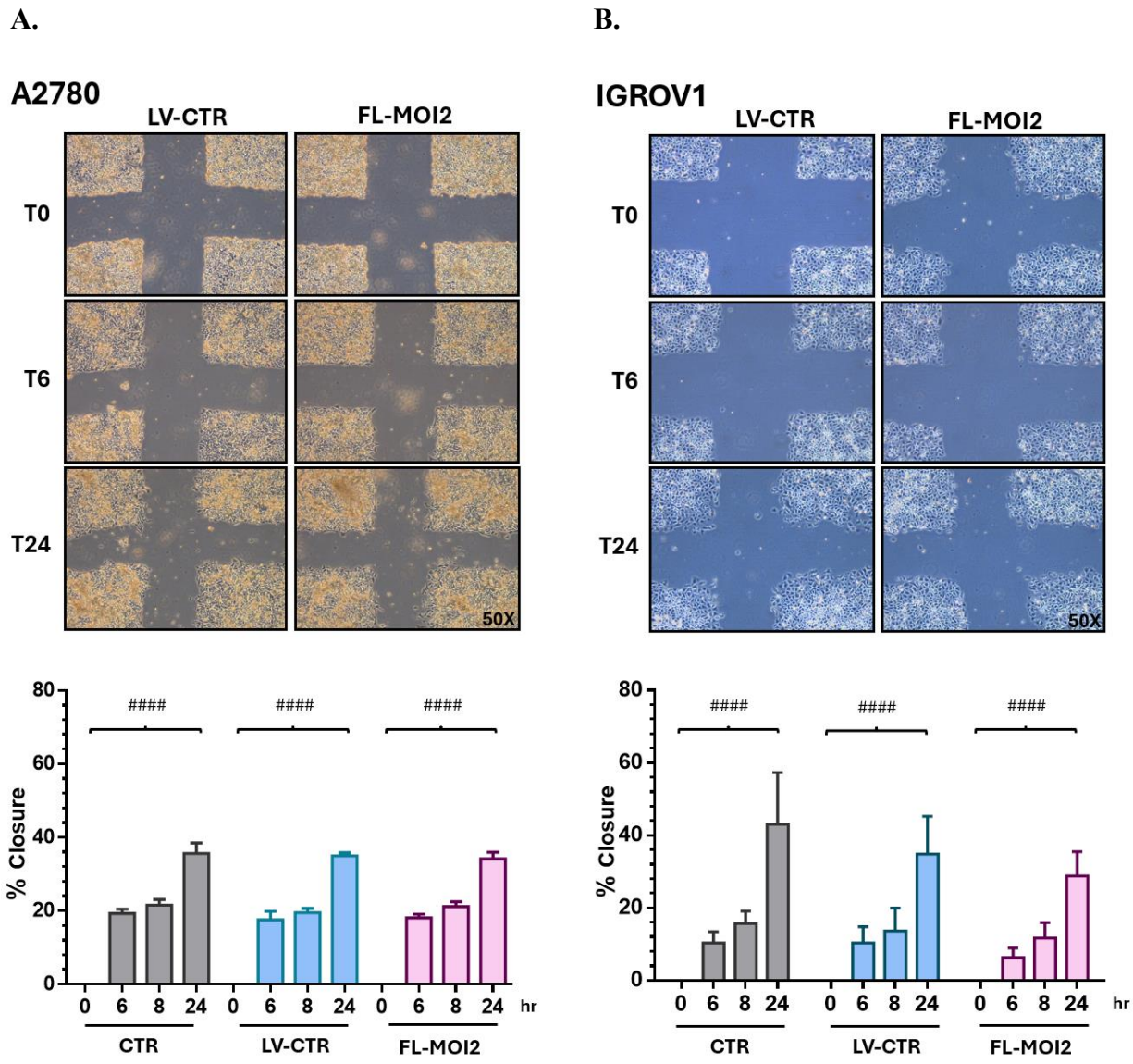


Figure 15. Cancer cell-derived FVIII-FL production does not influence ovarian cancer cell migration. *(A) Representative bright-field images and quantification (% Closure) of the wound area in A2780 cells at T0, 6, and 24 hrs, for CTR, LV-CTR and FL-MOI2 in 0.5% FBS. Magnification, 50×. (B) Representative bright-field images and quantification (% Closure) of the wound area in IGROV1 cells at T0, 6, and 24 hrs, for CTR, LV-CTR and FL-MOI2 in 0.5% FBS. Magnification, 50×.*

5.3.3 Cell-derived FL-FVIII has a cell line specific effect on long-term cell survival

To assess the effect of cell-derived FL-FVIII on long-term cell survival, A2780 and IGROV1 cells were cultured in 0.5% FBS and stained with a DNA stain, TO-PRO3, at day 7 to assess membrane integrity. Stain intensity was measured by live-cell-imaging for 24hrs and quantified as the average cellular integrated optical intensity (OCU; Figure 16A, B). Both high VCN A2780 and IGROV1 cell lines were included to provide further evidence of metabolic overloading. The results show for A2780 no significant effect on overall cell survival for cells producing FL-FVIII,

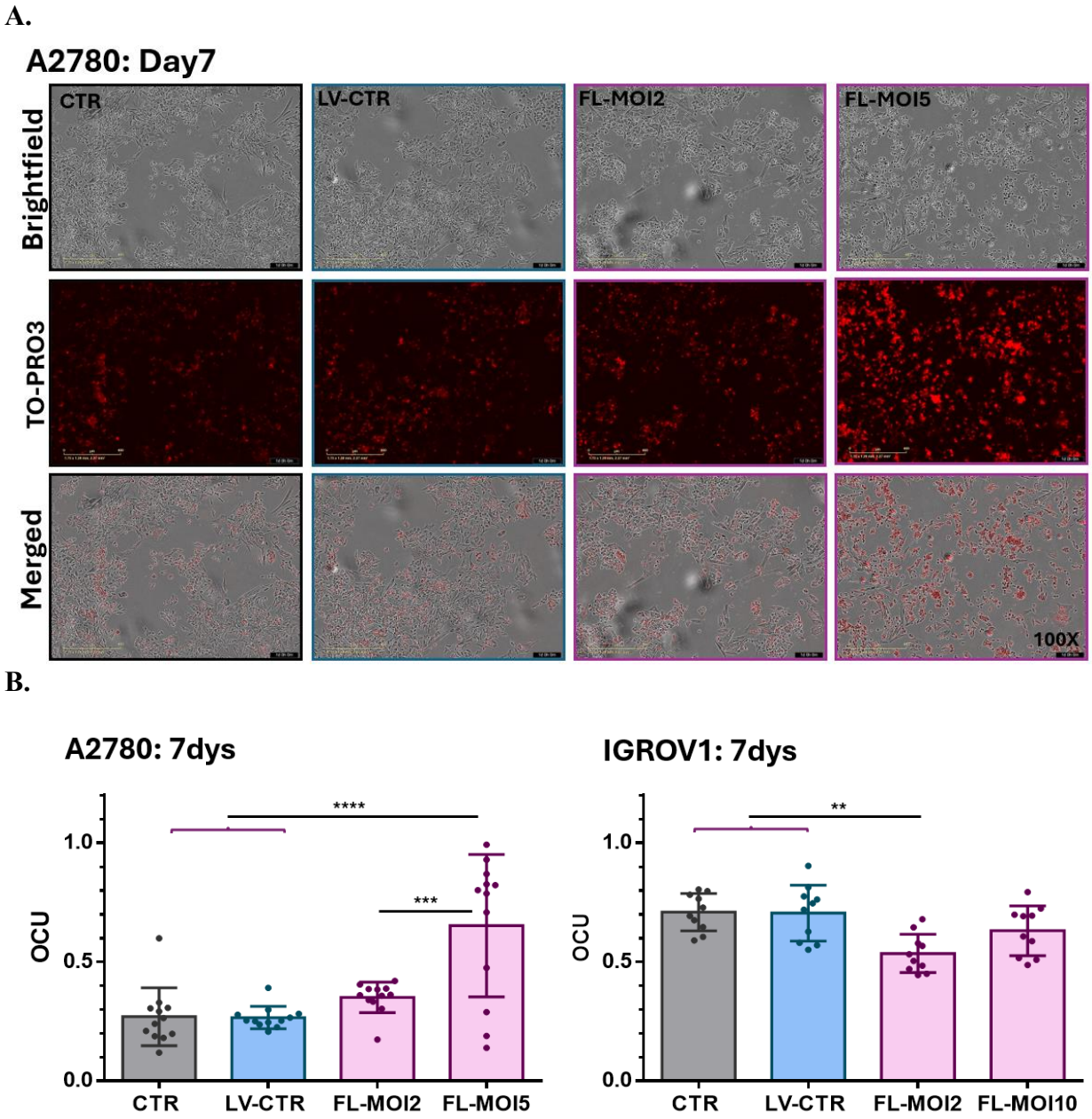


Figure 16. Cell-derived FL-FVIII has a cell line specific effect on overall cancer cell survival. *(A) Representative bright-field, TO-PRO-3 (DNA staining), and merged images of A2780 cells after 7 days in 0.5% FBS, showing CTR, LV-CTR, FL- MOI2, and FL-MOI5 (B) Quantification of the average cell TO-PRO-3 signal (OCU) in A2780 and IGROV1 cells at 7 days.*

while for IGROV1 a significant reduction in average OCU highlights an improved cell survival (Figure 16B). Considering those cells with a higher VCN, a significant decrease in cell survival was observed for A2780 while no impact was seen for IGROV1. Results overall highlight a differential effect of FL-FVIII according to the cell line investigated, suggesting that there is possibly a regulation of FL-FVIII functioning in a cell-specific way.

5.3.4 Cell-derived FL-FVIII shows cell type specific effects on single cell survival over the long-term

To assess the effect of cell-derived FL-FVIII on clonogenic potential of single cells, colony formation assays were performed on both A2780 and IGROV1 producing FL-FVIII (FL-MOI2) and LV-CTR control cells. High VCN cell lines were excluded from this analysis due to

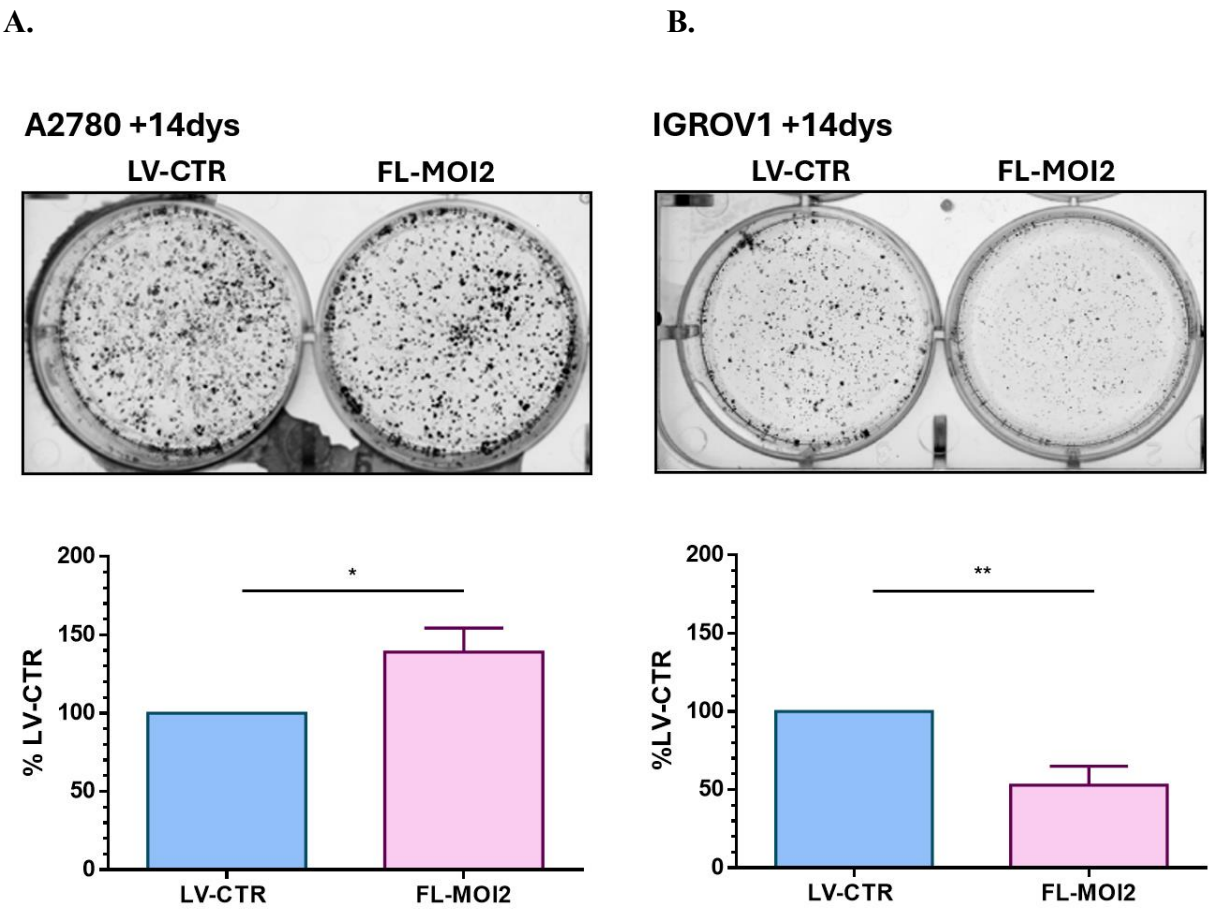


Figure 17. Cell-derived FL-FVIII shows a cell type specific effect on single cell colony formation over the long-term *(A) Representative scanned images of crystal violet-stained plates of the colony formation assay and quantification for A2780 cells, showing LV-CTR and FL-MOI2. (B) Representative scanned images of crystal violet-stained plates of the colony formation assay and quantification for IGROV1 cells, showing LV-CTR and FL-MOI2.*

suspected metabolic overloading. Colony counts based on pixel intensity were determined after 14dys with each compared to LV-CTR (set to 100%) to account for inter-experimental variation (Figure 17A, B). Results show that over the long-term colony formation based on staining intensity, were higher for A2780 FL-MOI2 cells, when compared to the LV-CTRs. Contrasting results, however, were observed for IGROV1, providing further evidence of a differential effect of FL-FVIII according to the cell line investigated.

5.4 Cell-specific signalling mechanisms observed in relationship to FL-FVIII production

To understand the differential cancer cell survival results observed for A2780 and IGROV1 cells chronically producing FL-FVIII (Sections 5.3.3, 5.3.4), previously investigated survival signalling pathways involved in recombinant FL-FVIII survival effects observed in bladder cancer cell lines (Walker et al., 2025), were analysed in the FL-MOI2 A2780 and IGROV1 cells cultured 24hrs in 0.5%FBS. Specific focus was given to integrins, players in the integrins signalling pathway and key survival proteins including Bcl2 and procaspase3. Further, given the well-established importance of TF in cancer progression and CAT, and the contrasting expression pattern between the two cell lines (Table 1), the protein expression of TF was also investigated as a potential player.

5.4.1 Cell-derived FL-FVIII production shows cell type-specific alterations for the integrin/FAK pathway as well as TF production

Cell lysates from CTR, LV-CTR and FL-FVIII continuously producing A2780 and IGROV1 (FL-MOI2) at 24hr in 0.5%FBS showed a differential pattern of integrin expression between cell lines and between the two different cell types. While expressing a similar α-integrin pattern for Intα5, α6 and αV between control cells and A2780 FL-MOI2 cells, cells producing FL-FVIII (FL-MOI2) had higher protein levels of β-Integrins, specifically Intβ1 and β3 (n=3; Figure 18A). IGROV1, on the other hand, showed no variation in the pattern of integrin expression, regardless of the production of FL-FVIII. They did, however, show a diverse β3 pattern to A2780 cells with a predominance of a lower molecular weight form, as opposed to the heavily glycosylated β3 form (Figure 18A). No regulation of integrin protein levels was not observed for IGROV1 with the production of FL-FVIII.

Of the ECM signalling proteins investigated that are downstream of integrins, both FAK and Src phosphorylation in FL-FVIII producing cells was more pronounced in both A2780 and IGROV1,

suggesting an elevated activation in both cell lines in relationship to FL-FVIII (Figure 18A). The pro-survival protein investigated, Bcl2, was only expressed by A2780 cells and was increased in FL-FVIII producing cells, while IGROV1 showed no Bcl2 expression. It remains to be understood the status of survival proteins in IGROV1 FL-MOI2 cells. Procaspase3 levels, however, were unchanged for both A2780 and IGROV1 continuously producing FL-FVIII. As expected, due to absence of TF mRNA, no TF protein was detected in A2780 cells or cells producing FL-FVIII (Figure 18A). In contrast, the IGROV1 cells expressed TF protein which importantly increased in FL-MOI2 cells (Figure 18A). Given TF is a transmembrane protein but known to be released in exosomes into the medium, media at 24hrs showed comparable TF levels likely related to the 0.5%FBS in CTR, LV-CTR and FL-MOI2 cells. These results highlight that FL-FVIII can promote TF production and its possible presence on the cell surface. Given that only whole cell lysates were investigated, it remains to be understood if elevated TF is localized to the membrane. Collectively, these results highlight that FL-FVIII production shows cell type-specific alterations in integrin/FAK pathway, as well as TF production (Figure 18B).

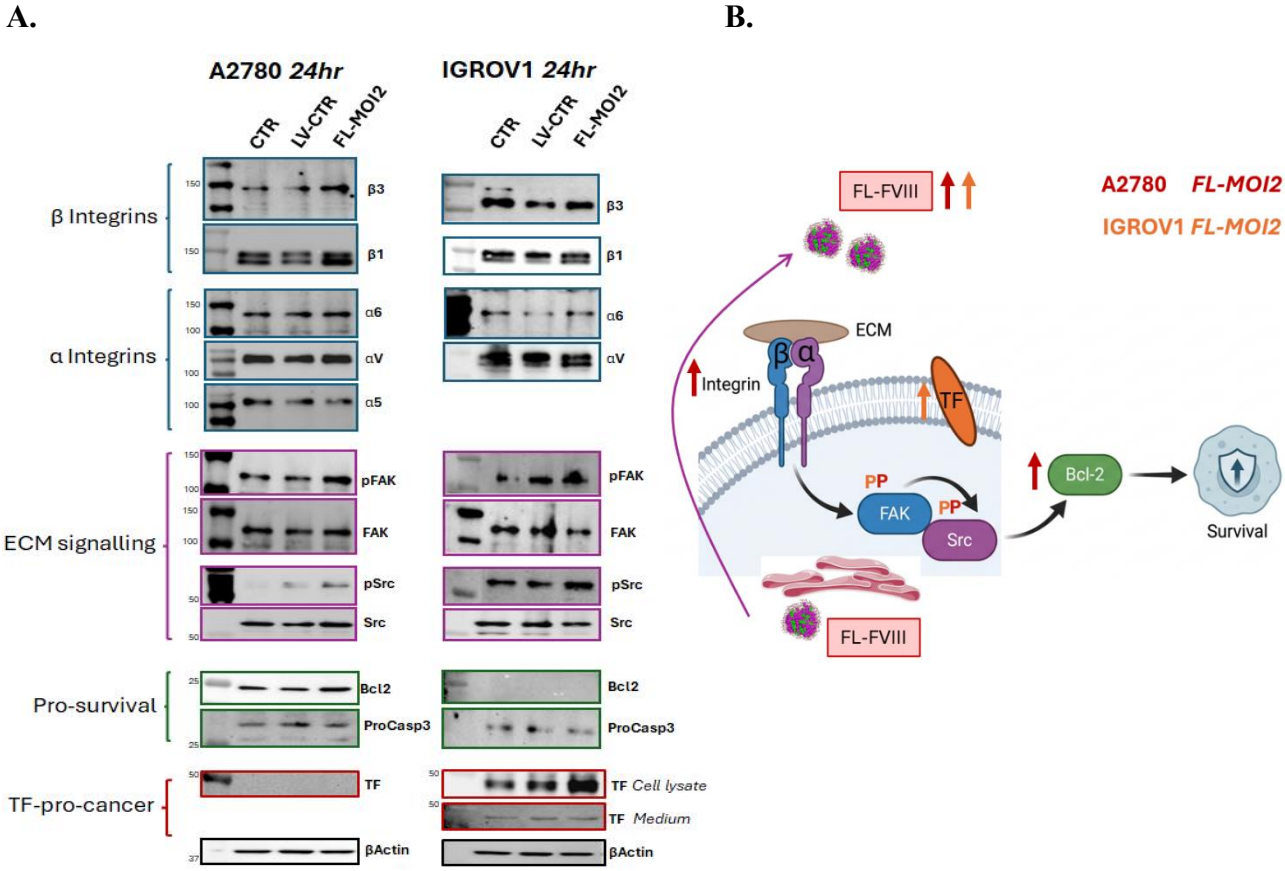


Figure 18. Cell-derived FL-FVIII shows a cell type specific regulation of integrin/FAK pathway and TF protein expression *(A) Representative western blots of 24hr whole cell lysates from A2780 and IGROV1 cells (CTR, LV-CTR and FL-MOI2) in 0.5%FBS. (B) Summary of western blot results for FL-FVIII producing cells (FL-MOI2) with respect to control cell lines (CTR, LV-CTR) showing potential players involved in FL-FVIII survival effects.*

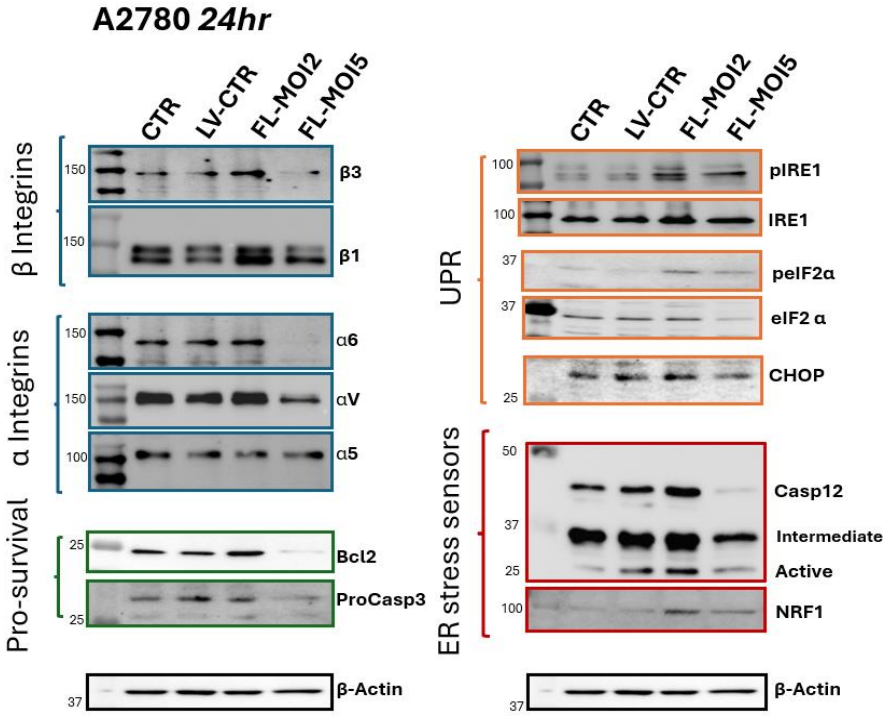
5.4.2 Higher FL-FVIII VCN in A2780 cancer cells causes endoplasmic reticulum (ER) stress and decreased Bcl2 survival protein expression

Based on the molecular characterization of FL-FVIII producing ovarian cancer cells in earlier experiments (Section 5.2.1), those cells with a VCN>4 (A2780 FL-MOI5, IGROV1 FL-MOI10) had a reduced mRNA expression and FL-FVIII protein production. Further, a significantly reduced proliferation over 24hrs was seen for both VCN>4 cell lines (Section 5.3.2.1), supporting metabolic overloading and ER stress, likely due to the processing of a large quantity of a large protein.

To confirm this, the A2780 cell FL-FVIII cell models with VCN≈2 (FL-MOI2) and >4 (FL-MOI5) and the corresponding controls (CTR, LV-CTR) were assessed by western blot for integrins and survival proteins (Bcl2, procaspase-3), as well as ER stress markers. The ER stress markers included of the 3 canonical players in the unfolded protein response (UPR) Inositol-requiring enzyme 1α (IRE1α), a downstream target of the second Protein kinase RNA-like ER kinase (PERK), *eukaryotic Translation Initiation Factor 2 subunit α (eIF2α)*, and for the third Activating transcription factor 6 (ATF6), the transcription factor *CHOP*. Further, two ER localized stress sensors, caspase-12 and nuclear factor erythroid 2-related factor 1 α (NRF1; driver of proteosome biogenesis with ER stress), were analyzed (Figure 19A, B).

Given that chronic ER stress is known to inhibit protein processing and trafficking of specific integrins to the plasma membrane (Contessa et al., 2008), at a high VCN (FL-MOI5) a decrease integrin β3 and α5, and a complete loss of α6, was observed highlighting a decrease in ECM interactions (Figure 19A, B). Further, a complete loss of the survival protein Bcl2 and a reduction in procaspase-3 in FL-MOI5 cells collectively support the process of anoikis. The presence of chronic ER stress in FL-MOI5 cells could be confirmed by an activated UPR, with an increased phosphorylation of both IRE1 (pIRE1) and eIF2α (peIF2α; Figure 19A, B). Contrary to what was expected based on an activated UPR, a decrease in the transcription factor CHOP was observed, likely regulated by other mechanisms. Similarly, in support of ER stress, the ER stress sensor caspase12 was in continuous cleavage and activation, while NRF1 protein levels were increased to increase proteosome production, supporting metabolic overloading and ER stress. It should be noted, that similar results were also observed for VCN≈2 (FL-MOI2) including UPR activation, an increase in total caspase12 and an increase in NRF1, highlighting that despite an increase in FL-FVIII production cell-derived pathophysiological effects, the processing of FL-FVIII impacts on ER homeostasis, likely due to the heavy processing of a large protein.

A.



B.

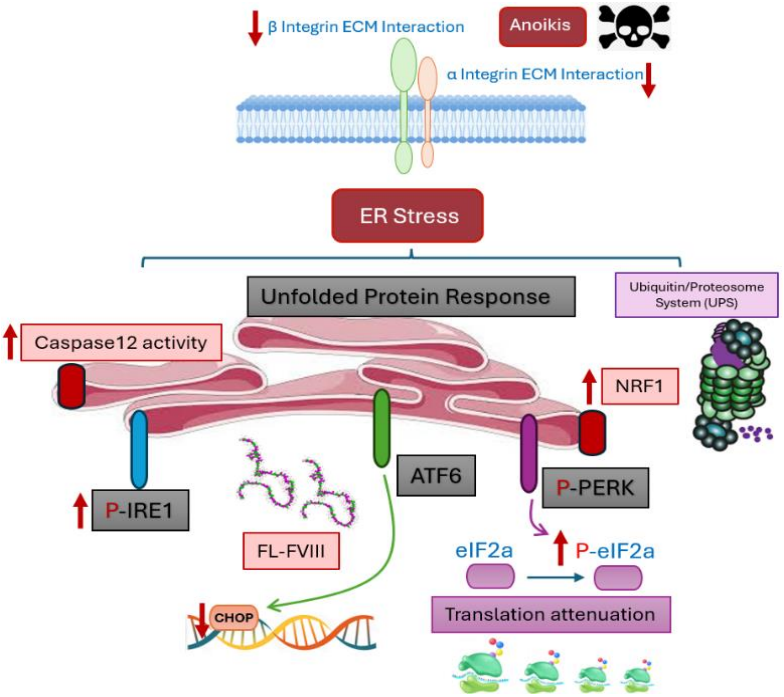


Figure 19. ER stress activated by FL-FVIII production in A2780 cells. *(A) Representative western blots from n=3 repeats of A2780 cells (CTR, LV-CTR, FL-MOI2, FL-MOI5) examining integrins, survival markers, UPR and ER stress sensors. (B) Schematic representation of the results highlighting the canonical markers of UPR and ER stress sensors activated by LV-FL-FVIII production.*

6. DISCUSSION

Cancer associated thrombosis is one of the most common and serious complications of cancer being the second leading cause of morbidity and mortality in patients (Sheth *et al*., 2017; Crobach *et al*., 2023; Soto Alsar *et al*., 2024). This clinical manifestation led to the hypothesis of coagulation factors playing a direct role in cancer, which was shortly followed by demonstrations of an upregulation of TF in cancer cells and its ability to regulate cancer cell proliferation, migration and survival (Hisada and Mackman, 2021; Unruh and Horbinski, 2020). Factor VIII has long been regarded as an important risk factor of cancer-related hypercoagulability, however, not an active one in tumour biology (Timp *et al*., 2015; Rietveld *et al*., 2019; Edvardsen *et al*., 2025). This conception, however, is changing due to the observation that different types and stages of human cancer and cancer cell lines, including, amongst others, thyroid, lung, breast, colon, bone, and bladder, have an mRNA expression profile second only to TF and that cancer cells secrete bioactive FVIII (Walker et al., 2022). An examination of the FVIII secretion profile from cancer cells of different origins, surprisingly highlighted the repeated presence of FL-FVIII, given that processing is intracellular (Walker et al. 2022). With the demonstration that recombinant FL-FVIII administration can contribute to cell cycle progression, migration, and most importantly, cancer cell survival in bladder cancer cell lines (Walker et al. 2025), suggested that cancer cell-derived FL-FVIII could potentially be an active player in tumor biology.

This study, aimed at investigating further the cell derived production of FL-FVIII using a LV delivery approach to increase the gene copy number and therefore FVIII production. Using two ovarian cell lines, A2780 and IGROV1, with low FVIII and differential TF production, both VCN and cell-type related differences were demonstrated. Continuous expression from high VCN cells impacted negatively on FL-FVIII production, proliferation and overall survival in both cell lines corresponding with chronic ER stress and UPR activation. In contrast, the lower FL-FVIII VCN successfully increased cell-derived FL-FVIII production in both cell lines augmenting single cell replication in A2780 by activating the integrin/FAK/Src signalling and increasing the levels of the survival protein, Bcl2. For IGROV1, overall cancer cell survival increased along with prothrombotic characteristics through an increase in TF, likely on the cell surface. Despite evidence of a role for cell-derived FL-FVIII in tumor biology, production even at the lower VCN also coincided with an increase in ER stress sensors and UPR activation, highlighting the model system overall as inappropriate for investigating the role of cell-derived FL-FVIII in tumorigenesis.

Given the size of FL-FVIII (≈330 kDa; vector insert size of 14,821 bp), it was anticipated that transduction itself might be difficult, since standard LV vectors are typically packaged with high efficiency only up to 10 kb, and payloads approaching or exceeding this are prone to reduced integration (Kumar et al., 2001). This, however, was not the case: transduction was successfully achieved, consistent with groups claiming that LV vectors have no strict absolute packaging limit, with integration obtainable even for proviral lengths exceeding 18 kb (Napoleone et al. 2026). With the VCN in the present study increasing with MOI, transduction and integration were excluded as the limiting steps. For the higher VCNs in both cell lines, a decrease in FVIII transcription and translation was evident, suggesting "metabolic overloading" causing an overall attenuation (Chen et al., 2023). The FL-FVIII protein is ≈330kDa and heavily glycosylated (Kumar et al., 2001). With a continuous transcription and translation of FL-FVIII, the ER may not be able to fold and process such a large and complex glycoprotein in increased quantities. This saturation activates UPR mechanisms which aim at preventing the toxicity of proteins. One mechanism is attenuation of global translation by phosphorylation of eIF2α, as was seen in A2780 cells. Early ‘adaptive’ and ‘compensatory’ responses which lead to an ‘apoptotic death switch' is caspase-12 (a resident of the ER) activation which increases the activity of the executioner caspase-3 and caspase-9 (Tabas and Ron, 2011). This mirrors what is seen in high FL-FVIII VCN cancer cells, where constant cleavage of caspase-12 was observed, supported by a decrease in procaspase3 due to its activation by cleavage, and the complete loss of the survival protein Bcl2. Further, the simultaneous rise in NRF1 in the high VCN cells, promotes the expression of proteasome subunits, suggesting that the cells are coping with the misfolded-protein burden by trying to increase the expression of protein-degrading enzymes (Radhakrishnan et al., 2012). Surprisingly, the transcription factor CHOP was reduced in high VCN cells, in contrast to expectations (Tabas and Ron, 2011). Given its known role in ER stress-induced apoptosis, it may be down regulated with the attenuation of translation following chronic UPR activation, as seen in other models (Woo et al., 2012).

Despite the clear limitations of the model, with even low VCNs (VCN≈2) activating the UPR, suggestive pro-tumorigenic effects from FL-FVIII production in both cell lines were still observed. The continuous FL-FVIII production at low VCNs, increased integrin protein levels and the phosphorylation of FAK and Src, despite clear evidence of the activation of ER stress sensors and UPR. The non-receptor tyrosine kinases, FAK and Src, associate at the focal adhesion to act together to regulate survival, proliferation and invasion through integrin and growth factor receptor signalling (Mitra and Schlaepfer, 2006). Activation of this pathway

increases survival and Bcl2 levels, either by the PI3K/Akt or the Ras/Raf/MEK/ERK pathways (Datta et al., 1997). While cellular adaptability to UPR may explain the FAK/Src signalling (Pugazhenthi et al., 2000), the single cell proliferative capability and survival experiments support a direct FL-FVIII effect. Further, these results are consistent with the observation that recombinant FL-FVIII modulates pro-survival pathways in bladder and bone cancer *in vitro* cell models (Walker et el., 2025).

Tissue factor is the main trigger of the extrinsic pathway of the coagulation cascade, and is often excessively produced in cancer, contributing to both systemic and local tumor progression by activation of protease-activated receptors (PARs; Koizume and Miyagi, 2022). An important observation was the significant increase in cellular TF of IGROV1 cells producing FL-FVIII, potentially enhancing their pro-thrombotic phenotype. Although FL-FVIII production failed to induce TF in the A2780 cells, this was expected since A2780 cells do not express TF (Sasano et. 2021). It is also important to note that TF levels in the conditioned media did not change, suggesting that the increase in cellular TF was not yet reflected in increased extracellular/exosomal release, an important characteristic of TF function (Hisada et al., 2022). While TF depends on PAR-2 for signalling, it also activates a second pathway associated with direct binding of its cytoplasmic and extracellular domains to integrins, particularly α3β1, which leads to cytoskeletal reorganisation and cell migration (Enjalbert et al., 2003). The functional consequences of increased TF levels by FL-FVIII, both pro-thrombotic and pathophysiological, remain to be determined.

Considering the ER stress and UPR activation at low a VCN with LV-FL-FVIII, alternate approaches should be addressed. The simplest approach would be to transduce with an MOI1, therefore increasing by only one copy and testing immediately for ER stress sensors such as caspase12 and NRF1. If successful, a similar approach evaluating the pathophysiological effects could be tested. Another approach would be to reduce the ER stress threshold. The use of a chemical chaperone, that increases the transport from the ER to the Golgi while not adding to the ER chaperone burden, such as betaine (Jeon et al.,2022). Betaine has been shown to increase the secretion of FVIII from CHO cells, by increasing the solubility of ER-bound FVIII aggregates, increasing the plasma level of FVIII in FVIII-knockout mice after gene transfer (Roth et al., 2012). This might be a possible method to consider for FL-FVIII, where higher levels of FL-FVIII can be secreted without triggering the UPR. Another approach could be to push the endogenous production, reducing the complications associated to randomly incorporating exogenous copies to the hosts genome. This involves the use of LV- Clustered Regularly

Interspaced Short Palindromic Repeats (CRISPR) Activation (LV-CRISPRa), a system that pushes your target gene at its native locus (Chavez et al., 2015). It has already been applied directly to coagulation factor genes, with Pignani et al., (2019) using a dCas9-VPR/sgRNA system to transactivate the promoters of F7 and F8, resulting in up to 35-fold increase in F7 promoter activity, and ~38-fold increase in F8 promoter activity in reporter assays, which equates to several-fold increase in endogenous FVII secretion (Pignani et al., 2019). In the ovarian cancer cell model used herein, this CRISPRa strategy could be applied to FL-FVIII, slowly incrementing the expression level from the native locus instead of high VCN LV integration, thereby avoiding metabolic overloading and the triggering of the UPR observed with the current LV approach, but allowing native transcriptional and post-translational regulation to proceed.

In summary, this work provides preliminary evidence supporting a potential role for cell-derived FL-FVIII in the biology of the cancer cells, despite the demonstration that LV model is inappropriate due to UPR activation and ER stress. Low FL-FVIII VCNs in both cell lines resulted in FAK/Src activation, impacting on different downstream pathways leading to an increase of the survival protein Bcl2 in A2780 cells, while promoting cellular TF production in IGROV1 cells. This lends to the notion that FL-FVIII could have multiple roles in tumour biology depending on the context of hosts expression and signalling profile. Alternative strategies are needed to raise the production of FL-FVIII without overloading the secretory pathway, such as chemical chaperone supplementation or trans-activation of the endogenous locus by CRISPRa. These methodologies may enable the pro-tumorigenic role of cell-derived FL-FVIII to be tested more cleanly and to establish its role as a player in the progression of cancer.

7. REFERENCES

Akinbo, D. B., and Ajayi, O. I. (2023). Thrombotic pathogenesis and laboratory diagnosis in cancer patients, an update. *International Journal of General Medicine*, 16, 259–272. https://doi.org/10.2147/IJGM.S385772

Al-Koussa, H., AlZaim, I., and El-Sabban, M. E. (2022). Pathophysiology of coagulation and emerging roles for extracellular vesicles in coagulation cascades and disorders. *Journal of Clinical Medicine*, 11(16), 4932. https://doi.org/10.3390/jcm11164932

Banerjee, D. K., Oliveira, C. M., Tavárez, J. J., Katiyar, V. N., Saha, S., Martínez, J. A., Banerjee, A., Sánchez, A., and Baksi, K. (2011). Importance of a factor viiic-like glycoprotein expressed in capillary endothelial cells (Efactor viiic) in angiogenesis. In A. M. Wu (Ed.), *The Molecular Immunology of Complex Carbohydrates-3* (Vol. 705, pp. 453–464). Springer US. https://doi.org/10.1007/978-1-4419-7877-6_24

Belting, M., Dorrell, M. I., Sandgren, S., Aguilar, E., Ahamed, J., Dorfleutner, A., Carmeliet, P., Mueller, B. M., Friedlander, M., and Ruf, W. (2004). Regulation of angiogenesis by tissue factor cytoplasmic domain signaling. *Nature Medicine*, 10(5), 502–509. https://doi.org/10.1038/nm1037

Bourcy, M., Suarez-Carmona, M., Lambert, J., Francart, M.-E., Schroeder, H., Delierneux, C., Skrypek, N., Thompson, E. W., Jérusalem, G., Berx, G., Thiry, M., Blacher, S., Hollier, B. G., Noël, A., Oury, C., Polette, M., and Gilles, C. (2016). Tissue factor induced by epithelial–mesenchymal transition triggers a procoagulant state that drives metastasis of circulating tumor cells. *Cancer Research*, 76(14), 4270–4282. https://doi.org/10.1158/0008-5472.CAN-15-2263

Boutilier, A. J., and Elsawa, S. F. (2021). Macrophage polarization states in the tumor microenvironment. *International Journal of Molecular Sciences*, 22(13), 6995. https://doi.org/10.3390/ijms22136995

Bray, F., Laversanne, M., Sung, H., Ferlay, J., Siegel, R. L., Soerjomataram, I., and Jemal, A. (2024). Global cancer statistics 2022: GLOBOCAN estimates of incidence and mortality worldwide for 36 cancers in 185 countries. *CA: A Cancer Journal for Clinicians*, *74*(3), 229–263. https://doi.org/10.3322/caac.21834

Cadé, M., Muñoz-Garcia, J., Babuty, A., Fouassier, M., Heymann, M.-F., Monahan, P. E., and Heymann, D. (2022). FVIII at the crossroad of coagulation, bone and immune biology: Emerging evidence of biological activities beyond hemostasis. *Drug Discovery Today*, *27*(1), 102–116. https://doi.org/10.1016/j.drudis.2021.07.015

Caliogna, L., Berni, M., Gastaldi, G., Grassi, F. A., Jannelli, E., Mosconi, M., Salatin, E., Burelli, S., Toninato, R., Pressacco, M., and Pasta, G. (2025). Trabecular titanium architecture drives human mesenchymal stem cell proliferation and bone differentiation. *International Journal of Molecular Sciences*, *26*(13), 6354. https://doi.org/10.3390/ijms26136354

Chanakira, A., Westmark, P. R., Ong, I. M., and Sheehan, J. P. (2017). Tissue factor-factor VIIa complex triggers protease activated receptor 2-dependent growth factor release and migration in ovarian cancer. *Gynecologic Oncology*, 145(1), 167–175. https://doi.org/10.1016/j.ygyno.2017.01.022

Chavez, A., Scheiman, J., Vora, S., Pruitt, B. W., Tuttle, M., P R Iyer, E., Lin, S., Kiani, S., Guzman, C. D., Wiegand, D. J., Ter-Ovanesyan, D., Braff, J. L., Davidsohn, N., Housden, B. E., Perrimon, N., Weiss, R., Aach, J., Collins, J. J., and Church, G. M. (2015). Highly efficient Cas9-mediated transcriptional programming. *Nature Methods*, 12(4), 326–328. https://doi.org/10.1038/nmeth.3312

Chen, Z., Herzog, R. W., and Kaufman, R. J. (2023). Cellular stress and coagulation factor production: When more is not necessarily better. *Journal of Thrombosis and Haemostasis*, 21(12), 3329–3341. https://doi.org/10.1016/j.jtha.2023.10.005

Claussen, C., Rausch, A.-V., Lezius, S., Amirkhosravi, A., Davila, M., Francis, J. L., Hisada, Y. M., Mackman, N., Bokemeyer, C., Schmalfeldt, B., Mahner, S., and Langer, F. (2016). Microvesicle-associated tissue factor procoagulant activity for the preoperative diagnosis of ovarian cancer. *Thrombosis Research*, 141, 39–48. https://doi.org/10.1016/j.thromres.2016.03.002

Contessa, J. N., Bhojani, M. S., Freeze, H. H., Rehemtulla, A., and Lawrence, T. S. (2008). Inhibition of n-linked glycosylation disrupts receptor tyrosine kinase signaling in tumor cells. *Cancer Research*, 68(10), 3803–3809. https://doi.org/10.1158/0008-5472.CAN-07-6389

Cottonaro, A., Akula, S., Pollio, B., Ricca, I., Martini, T., Albiani, R., Giacchello, J. A., Sciancalepore, P., Santi, R., Follenzi, A., and Merlin, S. (2026). Myeloid cell function and cytokine profiles in paediatric haemophilia a: Insights from fviii and emicizumab prophylaxis. *Journal of Cellular and Molecular Medicine*, *30*(11), e71216. https://doi.org/10.1111/jcmm.71216

Crobach, M. J. T., Anijs, R. J. S., Brækkan, S. K., Severinsen, M. T., Hammerstrøm, J., Skille, H., Kristensen, S. R., Paulsen, B., Tjønneland, A., Versteeg, H. H., Overvad, K., Hansen, J.-B., Næss, I. A., and Cannegieter, S. C. (2023). Survival after cancer-related venous thrombosis: The Scandinavian Thrombosis and Cancer Study. *Blood Advances*, 7(15), 4072–4079. https://doi.org/10.1182/bloodadvances.2022009577

Datta, S. R., Dudek, H., Tao, X., Masters, S., Fu, H., Gotoh, Y., and Greenberg, M. E. (1997). Akt phosphorylation of BAD couples survival signals to the cell-intrinsic death machinery. *Cell*, 91(2), 231–241. https://doi.org/10.1016/S0092-8674(00)80405-5

De Pablo-Moreno, J. A. D., Serrano, L. J., Revuelta, L., Sánchez, M. J., and Liras, A. (2022). The vascular endothelium and coagulation: Homeostasis, disease, and treatment, with a focus on the von Willebrand factor and factors viii and v. *International Journal of Molecular Sciences*, 23(15), 8283. https://doi.org/10.3390/ijms23158283

Dorner, A. J., Bole, D. G., and Kaufman, R. J. (1987). The relationship of N-linked glycosylation and heavy chain-binding protein association with the secretion of glycoproteins. *The Journal of Cell Biology*, 105(6), 2665–2674. https://doi.org/10.1083/jcb.105.6.2665

Edvardsen, M. S., Hansen, E.-S., Ueland, T., Latysheva, N., Aukrust, P., Snir, O., Morelli, V. M., and Hansen, J.-B. (2025). Effect of plasma levels of factor VIII according to procoagulant phospholipids on the risk of future venous thromboembolism. *Research and Practice in Thrombosis and Haemostasis*, 9(1), 102636. https://doi.org/10.1016/j.rpth.2024.102636

Enjalbert, B., Nantel, A., and Whiteway, M. (2003). Stress-induced gene expression in candida albicans: Absence of a general stress response. *Molecular Biology of the Cell*, 14(4), 1460–1467. https://doi.org/10.1091/mbc.e02-08-0546

Fahs, S. A., Hille, M. T., Shi, Q., Weiler, H., and Montgomery, R. R. (2014). A conditional knockout mouse model reveals endothelial cells as the principal and possibly exclusive source of plasma factor VIII. *Blood*, 123(24), 3706–3713. https://doi.org/10.1182/blood-2014-02-555151

Falanga, A., Marchetti, M., Vignoli, A., and Balducci, D. (2003). Clotting mechanisms and cancer: Implications in thrombus formation and tumor progression. *Clinical Advances in Hematology and Oncology*, 1(11), 673–678. PMID: 16258469.

Falanga, A., Russo, L., and Verzeroli, C. (2013). Mechanisms of thrombosis in cancer. *Thrombosis Research*, 131, S59–S62. https://doi.org/10.1016/S0049-3848(13)70024-0

Fay, P. (2006). Factor viii structure and function. *International Journal of Hematology*, 83(2), 103–108. https://doi.org/10.1532/IJH97.05113

Follenzi, A., and Naldini, L. (2002). Generation of HIV-1 derived lentiviral vectors. *Methods in Enzymology*, 346, 454–465. https://doi.org/10.1016/s0076-6879(02)46071-5

Franchini, M., Montagnana, M., Favaloro, E., and Lippi, G. (2009). The bidirectional relationship of cancer and hemostasis and the potential role of anticoagulant therapy in moderating thrombosis and cancer spread. *Seminars in Thrombosis and Hemostasis*, *35*(07), 644–653. https://doi.org/10.1055/s-0029-1242718

Fulcher, C. A., Roberts, J. R., Holland, L. Z., and Zimmerman, T. S. (1985). Human factor VIII procoagulant protein. Monoclonal antibodies define precursor-product relationships and functional epitopes. *Journal of Clinical Investigation*, 76(1), 117–124. https://doi.org/10.1172/JCI111933

Goldsmith, G. H. (2001). Hemostatic changes in patients with malignancy. *International Journal of Hematology*, 73(2), 151–156. https://doi.org/10.1007/BF02981931

Graw, J., Brackmann, H.-H., Oldenburg, J., Schneppenheim, R., Spannagl, M., and Schwaab, R. (2005). Haemophilia A: From mutation analysis to new therapies. *Nature Reviews Genetics*, 6(6), 488–501. https://doi.org/10.1038/nrg1617

Haberichter, S. L., and O'Donnell, J. S. (2025). Structure and multiple functions of von Willebrand factor. *Haematologica*, 111(1), 15–25. https://doi.org/10.3324/haematol.2024.286029

Hamer, R. J., Koedam, J. A., Beeser-Visser, N. H., Sixma, J. J., Bertina, R. M., and Mourik, J. A. (1987). Factor VIII binds to von Willebrand factor via its Mr-80000 light chain. *European Journal of Biochemistry*, 166(1), 37–43. https://doi.org/10.1111/j.1432-1033.1987.tb13480.x

Hisada, Y., and Mackman, N. (2021). Tissue factor and extracellular vesicles: Activation of coagulation and impact on survival in cancer. *Cancers*, 13(15), 3839. https://doi.org/10.3390/cancers13153839

Hisada, Y., Sachetto, A. T. A., and Mackman, N. (2022). Circulating tissue factor-positive extracellular vesicles and their association with thrombosis in different diseases. *Immunological Reviews*, 312(1), 61–75. https://doi.org/10.1111/imr.13106

Hui, S.-K. R. (2016). Hemophilia a, hemophilia b, congenital von willebrand disease, and acquired von willebrand syndrome. In J. Teruya (Ed.), *Management of Bleeding Patients* (pp. 77–84). Springer International Publishing. https://doi.org/10.1007/978-3-319-30726-8_7

Ivanciu, L., and Stalker, T. J. (2015). Spatiotemporal regulation of coagulation and platelet activation during the hemostatic response in vivo. *Journal of Thrombosis and Haemostasis*, 13(11), 1949–1959. https://doi.org/10.1111/jth.13145

Jeon, J.-H., Im, S., Kim, H. S., Lee, D., Jeong, K., Ku, J.-M., and Nam, T.-G. (2022). Chemical chaperones to inhibit endoplasmic reticulum stress: Implications in diseases. *Drug Design, Development and Therapy*, 16, 4385–4397. https://doi.org/10.2147/DDDT.S393816

Jun, Z., Ming-ming, L., Qian-qing, Z., Yun-hong, W., Chong-Yang, Z., and Xin, L. (2020). Functional identification of factor VIII B domain regions in hepatocyte cells. *Biochemical and Biophysical Research Communications*, 526(3), 633–640. https://doi.org/10.1016/j.bbrc.2020.03.132

Kaufman, R. J., Pipe, S. W., Tagliavacca, L., Swaroop, M., and Moussalli, M. (1997). Biosynthesis, assembly and secretion of coagulation factor VIII. *Blood Coagulation and Fibrinolysis*, 8(Suppl 2), S3–S14.

Klintman, J., Hillarp, A., Donfield, S., Berntorp, E., and Astermark, J. (2013). Antibody formation and specificity in Bethesda-negative brother pairs with haemophilia A. *Haemophilia*, 19(1), 106–112. https://doi.org/10.1111/j.1365-2516.2012.02903.x

Koizume, S., and Miyagi, Y. (2022). Tissue factor in cancer-associated thromboembolism: Possible mechanisms and clinical applications. *British Journal of Cancer*, 127(12), 2099–2107. https://doi.org/10.1038/s41416-022-01968-3

Kumar, M., Keller, B., Makalou, N., and Sutton, R. E. (2001). Systematic determination of the packaging limit of lentiviral vectors. *Human Gene Therapy*, 12(15), 1893–1905. https://doi.org/10.1089/104303401753153947

Kwaan, H. C., and Samama, M. (Eds.). (2019). *Clinical thrombosis* (1st ed.). CRC Press. https://doi.org/10.1201/9780429261879

Liu, J., Geng, X., Hou, J., and Wu, G. (2021). New insights into M1/M2 macrophages: Key modulators in cancer progression. *Cancer Cell International*, 21(1), 389. https://doi.org/10.1186/s12935-021-02089-2

Mantovani, A., and Locati, M. (2013). Tumor-associated macrophages as a paradigm of macrophage plasticity, diversity, and polarization: Lessons and open questions. *Arteriosclerosis, Thrombosis, and Vascular Biology*, 33(7), 1478–1483. https://doi.org/10.1161/ATVBAHA.113.300168

Mazurkiewicz-Pisarek, A., Płucienniczak, G., Ciach, T., and Płucienniczak, A. (2016). The factor VIII protein and its function. *Acta Biochimica Polonica*, 63(1). https://doi.org/10.18388/abp.2015_1056

Mitra, S. K., and Schlaepfer, D. D. (2006). Integrin-regulated FAK–Src signaling in normal and cancer cells. *Current Opinion in Cell Biology*, 18(5), 516–523. https://doi.org/10.1016/j.ceb.2006.08.011

Mohren, M., Jentsch-Ullrich, K., Koenigsmann, M., Kropf, S., Schalk, E., and Lutze, G. (2016). High coagulation factor VIII and von Willebrand factor in patients with lymphoma and leukemia. *International Journal of Hematology*, 103(2), 189–195. https://doi.org/10.1007/s12185-015-1913-y

Olgasi, C., Cucci, A., Molineris, I., Assanelli, S., Anselmi, F., Borsotti, C., Sgromo, C., Lauria, A., Merlin, S., Walker, G. E., Oliviero, S., and Follenzi, A. (2024). Factor VIII promotes angiogenesis and vessel stability regulating extracellular matrix proteins. *Haematologica*, *109*(10), 3391–3397. https://doi.org/10.3324/haematol.2024.285089

Pignani, S., Zappaterra, F., Barbon, E., Follenzi, A., Bovolenta, M., Bernardi, F., Branchini, A., and Pinotti, M. (2019). Tailoring the CRISPR system to transactivate coagulation gene promoters in normal and mutated contexts. *Biochimica et Biophysica Acta (BBA) - Gene Regulatory Mechanisms*, 1862(6), 619–624. https://doi.org/10.1016/j.bbagrm.2019.04.002

Prandoni, P., Falanga, A., and Piccioli, A. (2005). Cancer and venous thromboembolism. *The Lancet Oncology*, 6(6), 401–410. https://doi.org/10.1016/S1470-2045(05)70207-2

Prasannan, A., Venkatachalam, K., and Binesh, A. (2025). Factor VIII beyond haemophilia: A hidden regulator of venous thrombosis and endothelial dysfunction. *Blood Coagulation and Fibrinolysis*, 36(7), 335–346. https://doi.org/10.1097/MBC.0000000000001385

Pugazhenthi, S., Nesterova, A., Sable, C., Heidenreich, K. A., Boxer, L. M., Heasley, L. E., and Reusch, J. E.-B. (2000). Akt/protein kinase b up-regulates bcl-2 expression through camp-response element-binding protein. *Journal of Biological Chemistry*, 275(15), 10761–10766. https://doi.org/10.1074/jbc.275.15.10761

Repetto, O., and De Re, V. (2017). Coagulation and fibrinolysis in gastric cancer. *Annals of the New York Academy of Sciences*, 1404(1), 27–48. https://doi.org/10.1111/nyas.13454

Rhee, I. (2016). Diverse macrophages polarization in tumor microenvironment. *Archives of Pharmacal Research*, 39(11), 1588–1596. https://doi.org/10.1007/s12272-016-0820-y

Rietveld, I. M., Lijfering, W. M., Le Cessie, S., Bos, M. H. A., Rosendaal, F. R., Reitsma, P. H., and Cannegieter, S. C. (2019). High levels of coagulation factors and venous thrombosis risk: Strongest association for factor VIII and von Willebrand factor. *Journal of Thrombosis and Haemostasis*, 17(1), 99–109. https://doi.org/10.1111/jth.14343

Ron, D., and Walter, P. (2007). Signal integration in the endoplasmic reticulum unfolded protein response. *Nature Reviews Molecular Cell Biology*, 8(7), 519–529. https://doi.org/10.1038/nrm2199

Rosenberg, J. B., Foster, P. A., Kaufman, R. J., Vokac, E. A., Moussalli, M., Kroner, P. A., and Montgomery, R. R. (1998). Intracellular trafficking of factor VIII to von Willebrand factor storage granules. *Journal of Clinical Investigation*, 101(3), 613–624. https://doi.org/10.1172/JCI1250

Roth, S. D., Schüttrumpf, J., Milanov, P., Abriss, D., Ungerer, C., Quade-Lyssy, P., Simpson, J. C., Pepperkok, R., Seifried, E., and Tonn, T. (2012). Chemical chaperones improve protein secretion and rescue mutant factor viii in mice with hemophilia a. *PLoS ONE*, 7(9), e44505. https://doi.org/10.1371/journal.pone.0044505

Ruf, W., Yokota, N., and Schaffner, F. (2010). Tissue factor in cancer progression and angiogenesis. *Thrombosis Research*, 125, S36–S38. https://doi.org/10.1016/S0049-3848(10)70010-4

Saenko, E. L., Ananyeva, N. M., Tuddenham, E. G. D., and Kemball-Cook, G. (2002). Factor VIII – novel insights into form and function. *British Journal of Haematology*, 119(2), 323–331. https://doi.org/10.1046/j.1365-2141.2002.03793.x

Schaffner, F., and Ruf, W. (2009). Tissue factor and par2 signaling in the tumor microenvironment. *Arteriosclerosis, Thrombosis, and Vascular Biology*, 29(12), 1999–2004. https://doi.org/10.1161/ATVBAHA.108.177428

Sheth, R. A., Niekamp, A., Quencer, K. B., Shamoun, F., Knuttinen, M.-G., Naidu, S., and Oklu, R. (2017). Thrombosis in cancer patients: Etiology, incidence, and management. *Cardiovascular Diagnosis and Therapy*, 7(S3), S178–S185. https://doi.org/10.21037/cdt.2017.11.02

Soto Alsar, J., Jiménez Rodríguez, R., Gutiérrez, A., Ortega Morán, L., and Muñoz Martín, A. J. (2024). Update in venous thromboembolism in cancer: Lessons from multi-centre registries. *Thrombosis Update*, 16, 100183. https://doi.org/10.1016/j.tru.2024.100183

Tabas, I., and Ron, D. (2011). Integrating the mechanisms of apoptosis induced by endoplasmic reticulum stress. *Nature Cell Biology*, 13(3), 184–190. https://doi.org/10.1038/ncb0311-184

Tamura, R., Yoshihara, K., and Enomoto, T. (2022). Therapeutic strategies focused on cancer-associated hypercoagulation for ovarian clear cell carcinoma. *Cancers*, 14(9), 2125. https://doi.org/10.3390/cancers14092125

Thompson, A. R. (2003). Structure and function of the factor viii gene and protein. *Seminars in Thrombosis and Hemostasis*, 29(1), 011–022. https://doi.org/10.1055/s-2003-37935

Timp, J. F., Braekkan, S. K., Versteeg, H. H., and Cannegieter, S. C. (2013). Epidemiology of cancer-associated venous thrombosis. *Blood*, 122(10), 1712–1723. https://doi.org/10.1182/blood-2013-04-460121

Toole, J. J., Pittman, D. D., Orr, E. C., Murtha, P., Wasley, L. C., and Kaufman, R. J. (1986). A large region (Approximately equal to 95 kda) of human factor VIII is dispensable for in vitro procoagulant activity. *Proceedings of the National Academy of Sciences*, 83(16), 5939–5942. https://doi.org/10.1073/pnas.83.16.5939

Unruh, D., and Horbinski, C. (2020). Beyond thrombosis: The impact of tissue factor signaling in cancer. *Journal of Hematology and Oncology*, 13(1), 93. https://doi.org/10.1186/s13045-020-00932-z

Van Den Biggelaar, M., Bouwens, E. A. M., Voorberg, J., and Mertens, K. (2011). Storage of factor viii variants with impaired von willebrand factor binding in weibel-palade bodies in endothelial cells. *PLoS ONE*, 6(8), e24163. https://doi.org/10.1371/journal.pone.0024163

Walker, G. E., Borroni, E., Haider, R., Olgasi, C., Borsotti, C., and Follenzi, A. (2025). Factor VIII, a coagulation cofactor, is a relevant survival factor in bladder cancer cell lines. *Journal of Thrombosis and Haemostasis*, 23(11), 3466–3480. https://doi.org/10.1016/j.jtha.2025.03.002

Walker, G. E., Merlin, S., Zanolini, D., Vandoni, A., Volpe, A., Gaidano, G., Valente, G., Olivero, M., and Follenzi, A. (2022). Factor VIII as a potential player in cancer pathophysiology. *Journal of Thrombosis and Haemostasis*, 20(3), 648–660. https://doi.org/10.1111/jth.15611

Winther-Larsen, A., Sandfeld-Paulsen, B., and Hvas, A.-M. (2022). New insights in coagulation and fibrinolysis in patients with primary brain cancer: A systematic review. *Seminars in Thrombosis and Hemostasis*, 48(03), 323–337. https://doi.org/10.1055/s-0041-1733961

Woo, C. W., Kutzler, L., Kimball, S. R., and Tabas, I. (2012). Toll-like receptor activation suppresses ER stress factor CHOP and translation inhibition through activation of eIF2B. *Nature Cell Biology*, 14(2), 192–200. https://doi.org/10.1038/ncb2408

Yusupovna, M. I., Rakhmanovich, A. I., and Juraevna, U. G. (2025). The role of macrophages in cancer progression: M1, M2 subtypes, and their impact on tumor microenvironment. *International Journal of Innovative Research and Scientific Studies*, 8(3), 3960–3969. https://doi.org/10.53894/ijirss.v8i3.7423

Zanolini, D., Merlin, S., Feola, M., Ranaldo, G., Amoruso, A., Gaidano, G., Zaffaroni, M., Ferrero, A., Brunelleschi, S., Valente, G., Gupta, S., Prat, M., and Follenzi, A. (2015). Extrahepatic sources of factor VIII potentially contribute to the coagulation cascade correcting the bleeding phenotype of mice with hemophilia A. *Haematologica*, *100*(7), 881–892. https://doi.org/10.3324/haematol.2014.123117

Zhang, W., Wang, M., Ji, C., Liu, X., Gu, B., and Dong, T. (2024). Macrophage polarization in the tumor microenvironment: Emerging roles and therapeutic potentials. *Biomedicine and Pharmacotherapy*, 177, 116930. https://doi.org/10.1016/j.biopha.2024.116930

Zhou, Q., Wei, S., Wang, H., Li, Y., Fan, S., Cao, Y., and Wang, C. (2023). T cell-derived exosomes in tumor immune modulation and immunotherapy. *Frontiers in Immunology*, 14, 1130033. https://doi.org/10.3389/fimmu.2023.1130033

ACKNOWLEDGEMENTS

Completing this degree is one of the milestones I am most proud of, and I owe it entirely to the people who have carried me through this journey. I feel incredibly lucky to be surrounded by people who believed in me and kept me going, even on the days I didn't believe in myself.

First and foremost, I would like to thank my supervisor, Prof. Antonia Follenzi, for welcoming me into the Histology Lab and trusting me with such a fascinating project. Your guidance pushed me to think more critically and independently, and I grew so much as a researcher because of it. I will always admire your dedication to your work, and I am deeply grateful for the confidence you placed in me from the very beginning.

I am endlessly grateful to Dr. Gillian Walker. Calling you a co-supervisor would not do justice to how much you have supported me throughout this journey. You have taught me not just about research, but about life. You met every single one of my questions with patience, no matter how many times I asked, and you showed me how to find balance when everything felt overwhelming. You have helped me through my most difficult times, and that kindness was never confined to the lab. I don't know how I would have gotten through this without you.

I am grateful beyond words to my family and friends. Without my parents' unconditional love and support, none of this would have been possible. From the very first step of this journey, you believed in me even when I doubted myself. Even from thousands of miles aways your encouragement never once wavered. Every late-night call, every word of reassurance, every sacrifice you made so I could chase this dream. I carry all of it with me, and I owe this achievement to them as much as to myself.

Divya and Manasi have been my pillars throughout my life, and even more so during this journey; calling them friends would be an understatement. No matter the distance or the time difference, you two have always been just a call away, cheering me on through every high and talking me down from every low. You have celebrated my smallest wins as if they were your own and reminded me of my worth on the days, I forgot it myself. Everything good in me comes from my parents, and from you girls.

Shwetha and Keziya, my little found family. I don't think I would have stayed sane in this country without you. Moving to a new country alone is never easy, but you two made sure I never had to feel that loneliness for long. You have encouraged me, supported me, motivated me, and given me a safe space to break down whenever I needed to, no questions asked. From late-night talks that turned into laughter, to studying together, to exploring every corner of this country we could find, you girls have made a foreign place feel like home. You have seen me at my most stressed and my most joyful, and you loved me through both. I will always, always be grateful that I met you both.

Last but not least, I would like to thank all the members of histology department but especially, Zabiha, Emanuella, Baker, Ali, Roberta, and Vato, for welcoming me into the lab and making me feel confident and comfortable from day one. Thank you for being good to me and making lab fun for me.